

On the Capacity of MIMO Broadband Power Line Communications Channels

Nir Shlezinger, Roe Shaked, and Ron Dabora

Abstract

Communications over power lines in the frequency range above 2 MHz, commonly referred to as broadband (BB) power line communications (PLC), has been the focus of increasing research attention and standardization efforts in recent years. BB-PLC channels are characterized by a dominant colored non-Gaussian additive noise, as well as by periodic variations of the channel impulse response and the noise statistics. In this work we study the fundamental rate limits for BB-PLC channels by bounding their capacity while accounting for the unique properties of these channels. We obtain explicit expressions for the derived bounds for several BB-PLC noise models, and illustrate the resulting fundamental limits in a numerical analysis.

Index terms— Power line communications, MIMO systems, channel capacity.

I. INTRODUCTION

Power line communications (PLC) utilizes the existing power grid infrastructure for data transmission. Communications over power lines in the frequency range of 2 – 100 MHz and possibly beyond, commonly referred to as broadband (BB) PLC [1], has received a significant research attention which has supported the development of new standards aiming at facilitating communications at higher data rates [2]. Since the indoor power line physical infrastructure consists of three wires, it is possible to utilize multiple input ports and/or multiple output ports at terminals by transmitting and/or receiving over multiple differential wire pairs [3], thereby realizing multiple input-multiple output (MIMO) communications over BB-PLC channels. The increasing importance of BB-PLC as a high-speed communications medium constitutes a strong motivation for characterizing the fundamental rate limits of these channels and the associated optimal channel coding schemes.

Nir Shlezinger is with the Faculty of Electrical Engineering, Technion, Haifa, Israel (e-mail: nirshlezing@technion.ac.il). Roe Shaked and Ron Dabora are with the department of ECE, Ben-Gurion University, Be'er-Sheva, Israel (e-mail: shroee@post.bgu.ac.il; ron@ee.bgu.ac.il). This work was supported by the Israel Science Foundation under Grant 1685/16.

A major challenge in characterizing the capacity of BB-PLC channels, both for scalar and for MIMO scenarios, follows since the additive noise in BB-PLC systems is a superposition of several noise sources, including stationary noise, non-impulsive noise with periodic statistics, impulsive noise with periodic statistics, and impulsive noise with non-periodic statistics [1, Ch. 2.6]. The resulting overall BB-PLC noise is generally modeled as a non-Gaussian [4]–[9], temporally correlated [8]–[12], non-stationary [9], [13]–[16] process, and MIMO BB-PLC noise components at different output ports are typically assumed to be correlated [2], [3], [20]. The channel impulse response (CIR) in BB-PLC channels is typically modeled as a multipath channel [9], [17] with periodic variations [13], [18], [19], where the channel outputs typically contain crosstalk from other wires [2], [3], [21]–[23]. Common models for the marginal probability density function (PDF) of BB-PLC noise include the Nakagami- m distribution [4], the Middleton class A distribution [24], and the Gaussian mixture (GM) distribution [8], [25]. All these models characterize only the *marginal PDF* of the additive noise process, while the *complete statistics* of the noise process (i.e., the joint PDF of any finite set of sample times) has not been characterized. The temporal correlation of the *stationary* noise component is typically characterized via its power spectral density (PSD), for which various models have been proposed [10]–[12]. The statistics of the *periodic* noise component in BB-PLC is commonly modeled as a cyclostationary process, see [13], [14]. Lastly, the non-periodic impulsive noise component in BB-PLC was modeled in [15], [16] as a non-stationary process, where [15] modeled the arrival times of the impulses using a partitioned Markov chain, while [16] modeled these arrival times as a Poisson process.

To avoid the technical difficulties that arise when analyzing the capacity of BB-PLC channels using the accurate statistics of the noise, previous works which attempted to characterize the fundamental rate limits for this channel, used very simplified models which do not capture many of the special characteristics of the noise in BB-PLC channels: The work [10] evaluated the capacity of BB-PLC channels modeled as linear time-invariant (LTI) systems with additive colored stationary Gaussian noise; the work [26] modeled BB-PLC channels as linear periodically time-varying (LPTV) channels with additive white Gaussian noise (AWGN), and evaluated the achievable rate by using a transmission scheme which utilizes orthogonal frequency division multiplexing (OFDM) signalling; the work [7] modeled the noise of BB-PLC channels as a Middleton class A process and used the expression for the capacity of LTI channels with colored stationary Gaussian noise (see, e.g., [27, Eq. (9.97)]) to evaluate the capacity. As this expression

was derived for a stationary Gaussian noise, then naturally it does not apply to Middleton class A noise. We emphasize that all the works mentioned above, i.e., [7], [10], [26], derived expressions assuming *Gaussian noise*, while major works have concluded that the noise is non-Gaussian, see, e.g., [4], [8], [9]. We also note the work [28], which derived an approximate expression for the achievable rates when using Gaussian inputs and when using inputs with discrete amplitudes, for memoryless channels with additive GM noise, which were used for modelling communications in the presence of co-channel interference. Finally, we note that the capacity of PLC channels in the *narrowband* frequency range (0–500 kHz), modeled as additive noise channels in which the CIR is modeled as an LPTV filter and the noise is a cyclostationary Gaussian process, was derived in [29]. To the best of our knowledge, the fundamental limits for BB-PLC channels, accounting for their unique characteristics, including the *non-Gaussianity and the temporal correlation of the noise*, as well as *the periodic variations of the CIR and of the noise statistics*, have not been characterized to date. In this work we aim to address this gap.

Main Contributions: In this work we study the fundamental rate limits of discrete-time (DT) BB-PLC channels. We consider a general channel model accounting for a wide range of the characteristics of BB-PLC channels, in which the CIR is modeled as an LPTV filter, and the additive noise is modeled as a temporally correlated *non-Gaussian cyclostationary process*¹. Accordingly, we characterize an upper bound and two lower bounds on the capacity of these channels. We note that when the noise is not a Gaussian process, obtaining a closed-form expression for the capacity is generally a very difficult task, even for stationary and memoryless channels, and the common approach is to characterize upper and lower bounds on the capacity, see, e.g., [30, Ch. 7.4]. To facilitate the derivation, we first derive bounds on the capacity of a general LTI MIMO channel with additive *non-Gaussian stationary noise*. Then, we prove that the capacity of BB-PLC channels can be obtained from the capacity of non-Gaussian LTI MIMO channels by properly setting the parameters of the model, and finally we apply the bounds on the capacity of the latter model to obtain the bounds on the capacity of BB-PLC channels. This approach yields capacity bounds which depend on the PDF of the noise process *only through its entropy rate and autocorrelation function*. Consequently, our bounds can be obtained explicitly whenever the entropy rate and the autocorrelation function of the noise are known, or can be

¹Although the cyclostationary noise statistics does not fully capture the statistics of the non-stationary component of the BB-PLC noise, it is considered an adequate representation of the overall temporal variations of the statistics of the additive noise in BB-PLC, see, e.g., [14] and [2, Sec. III-F].

well-approximated. Next, we derive explicit expressions for the entropy rates for several noise models applicable to BB-PLC, and use them to explicitly characterize the capacity bounds. We also identify scenarios corresponding to known BB-PLC channel models, e.g., [4]–[6], [8], in which the capacity bounds depend only on the *marginal PDF* and the autocorrelation function of the noise. In such scenarios the bounds can be explicitly obtained even when the complete statistical characterization of the noise process is unknown. The proposed capacity bounds hold for any noise model and distribution. As an example of our results, we numerically evaluate the capacity for several BB-PLC noise models, including GM, Middleton Class A, and the less common Nakagami- m model. Our results demonstrate that, in the high signal-to-noise ratio (SNR) regime, the achievable rate of *cyclostationary Gaussian signaling* is within a small gap of capacity. We also clearly show that assuming the noise is Gaussian may result in significantly underestimating the capacity, and eventually, lead to the design of schemes whose achievable rates are considerably lower than the maximal bit rate that can be supported by the channel.

The rest of this paper is organized as follows: Section II details the problem formulation; Section III derives bounds on the capacity of BB-PLC channels; Section IV presents an application of the results to the characterization of the capacity for several common BB-PLC models which previously appeared in the literature; Section V presents numerical examples; Lastly, Section VI provides some concluding remarks. Detailed proofs of the results are provided in the appendix.

II. PROBLEM DEFINITION

A. Notations

We use upper-case letters, e.g., X , to denote random variables (RVs), lower-case letters, e.g., x , to denote deterministic values, and calligraphic letters, e.g., \mathcal{X} , to denote sets. Column vectors are denoted with boldface letters, e.g., \mathbf{x} for a deterministic vector and \mathbf{X} for a random vector; the i -th element of \mathbf{x} ($i \geq 0$) is denoted with $(\mathbf{x})_i$. We use Sans-Sarif fonts to denote matrices, e.g., A , the element at the i -th row and the j -th column of A is denoted with $(A)_{i,j}$, the all-zero $k \times l$ matrix is denoted with $0_{k \times l}$, and the $n \times n$ identity matrix is denoted with I_n . Complex conjugate, transpose, Hermitian transpose, Euclidean norm, stochastic expectation, covariance, differential entropy, and mutual information are denoted by $(\cdot)^*$, $(\cdot)^T$, $(\cdot)^H$, $\|\cdot\|$, $\mathbb{E}\{\cdot\}$, $\text{Cov}(\cdot)$, $h(\cdot)$, and $I(\cdot; \cdot)$, respectively, and we use a^+ to denote $\max\{0, a\}$, and $|\cdot|$ to denote the magnitude when applied to scalars, and the determinant when applied to matrices. The sets of non-negative integers, integers, and real numbers are denoted by \mathcal{N} , \mathcal{Z} , and \mathcal{R} , respectively. All logarithms are

taken to base-2. Lastly, for any sequence, possibly multivariate, $\mathbf{y}[i]$, $i \in \mathcal{Z}$, and integers $b_1 < b_2$, $\mathbf{y}_{b_1}^{b_2}$ denotes the column vector obtained by stacking $\left[(\mathbf{y}[b_1])^T, \dots, (\mathbf{y}[b_2])^T \right]^T$ and $\mathbf{y}^{b_2} \equiv \mathbf{y}_0^{b_2}$.

B. Definitions

In the work we make use of the following definitions:

Definition 1 (A MIMO channel with finite-memory). A DT $n_r \times n_t$ MIMO channel with finite memory consists of an input sequence $\mathbf{X}[i] \in \mathcal{R}^{n_t}$, $i \in \mathcal{N}$, an output sequence $\mathbf{Y}[i] \in \mathcal{R}^{n_r}$, $i \in \mathcal{N}$, an initial state vector $\mathbf{S}_0 \in \mathcal{S}_0$ of finite dimensions, and a sequence of PDFs $\left\{ p_{\mathbf{Y}^n | \mathbf{X}^n, \mathbf{S}_0}(\mathbf{y}^n | \mathbf{x}^n, \mathbf{s}_0) \right\}_{n=0}^{\infty}$.

Definition 2 (Code). An $[R, l]$ code with rate R and blocklength $l \in \mathcal{N}$ consists of: 1) A message set $\mathcal{U} \triangleq \{1, 2, \dots, 2^{lR}\}$. 2) An encoder e_l which maps each message $u \in \mathcal{U}$ into an $n_t \times l$ codeword matrix $\mathbf{X}_{(u)}^{l-1} \triangleq [\mathbf{x}_{(u)}[0], \mathbf{x}_{(u)}[1], \dots, \mathbf{x}_{(u)}[l-1]]$, where $\mathbf{x}_{(u)}[i]$ denotes the inputs at the n_t channel input ports at time i . 3) A decoder d_l which maps the channel output sequence $[\mathbf{y}[0], \mathbf{y}[1], \dots, \mathbf{y}[l-1]] \in \mathcal{R}^{n_r \times l}$ into a message $\hat{u} \in \mathcal{U}$. The encoder and decoder operate independently of the initial state, in the sense that \mathbf{S}_0 does not affect the encoding and the decoding operations.

The set $\left\{ \mathbf{X}_{(u)}^{l-1} \right\}_{u=1}^{2^{lR}}$ is referred to as the *codebook* of the $[R, l]$ code. Assuming the message U is uniformly selected from \mathcal{U} , the average probability of error, when the initial state is \mathbf{s}_0 , is:

$$P_e^l(\mathbf{s}_0) = \frac{1}{2^{lR}} \sum_{u=1}^{2^{lR}} \Pr(d_l(\mathbf{Y}^{l-1}) \neq u | U=u, \mathbf{S}_0=\mathbf{s}_0).$$

Definition 3 (Achievable rate). A rate R_c is called *achievable* if, for every $\epsilon_1, \epsilon_2 > 0$, there exists a positive integer $l_0 > 0$ such that for all integer $l > l_0$, there exists an $[R, l]$ code which satisfies $\sup_{\mathbf{s}_0 \in \mathcal{S}_0} P_e^l(\mathbf{s}_0) < \epsilon_1$, and $R \geq R_c - \epsilon_2$.

Definition 4 (Capacity). *Capacity* is defined as the supremum of all achievable rates.

C. Model and Problem Formulation

We consider a DT $\tilde{n}_r \times \tilde{n}_t$ MIMO BB-PLC channel with \tilde{n}_r receive ports and \tilde{n}_t transmit ports, modeled as a multivariate LPTV system with additive non-Gaussian cyclostationary noise². Let

²In the following, we use the tilde notation for quantities associated with the MIMO BB-PLC channel, highlighting the fact that this is a periodic channel model. The same notations without a tilde represent the corresponding quantities associated with the linear non-Gaussian MIMO channel defined in Subsection III-A, which is a non-periodic channel model.

\tilde{m} be a non-negative integer which represents the *length of the memory of the channel*, \tilde{p}_G be a positive integer which represents the *period of the CIR*, and \tilde{p}_W be a positive integer which represents the *period of the noise statistics*. Let $\tilde{\mathbf{W}}[i] \in \mathcal{R}^{\tilde{n}_r}$ be a real-valued \tilde{n}_r -dimensional zero-mean strict-sense cyclostationary non-Gaussian additive noise³, i.e., for any set of k integer indexes $\{i_l\}_{l=1}^k$, $k \in \mathcal{N}$, the joint PDF of $\tilde{\mathbf{W}}[i_1], \tilde{\mathbf{W}}[i_2], \dots, \tilde{\mathbf{W}}[i_k]$ is equal to the joint PDF of $\tilde{\mathbf{W}}[i_1 + \tilde{p}_W], \tilde{\mathbf{W}}[i_2 + \tilde{p}_W], \dots, \tilde{\mathbf{W}}[i_k + \tilde{p}_W]$. Since the channel memory is \tilde{m} , then noise vectors more than \tilde{m} instances apart are mutually independent, i.e., $\forall i_1, i_2, l_1, l_2 \in \mathcal{N}$ such that $i_2 > i_1 + l_1 + \tilde{m}$, the random vectors $\tilde{\mathbf{W}}_{i_1}^{i_1+l_1}$ and $\tilde{\mathbf{W}}_{i_2}^{i_2+l_2}$ are mutually independent. We further assume that there is no deterministic dependence between instances of $\tilde{\mathbf{W}}[i]$, i.e., $\nexists i_0$ for which $\tilde{\mathbf{W}}[i_0]$ can be expressed as a linear combination of $\{\tilde{\mathbf{W}}[i]\}_{i \neq i_0}$. Let $\{\tilde{G}[i, \tau]\}_{\tau=0}^{\tilde{m}}$ denote the LPTV CIR. The periodicity of the CIR implies that $\tilde{G}[i, \tau] = \tilde{G}[i + \tilde{p}_G, \tau]$, $\forall i \in \mathcal{Z}, \tau \in \{0, 1, \dots, \tilde{m}\}$.

With the above definitions, the input-output relationship for the MIMO BB-PLC channel with input codeword length \tilde{l} is given by

$$\tilde{\mathbf{Y}}[i] = \sum_{\tau=0}^{\tilde{m}} \tilde{G}[i, \tau] \tilde{\mathbf{X}}[i - \tau] + \tilde{\mathbf{W}}[i], \quad i \in \{0, 1, \dots, \tilde{l} - 1\}, \quad (1)$$

where the initial state of the channel (i.e., prior to the beginning of reception) is given by $\tilde{\mathbf{S}}_0 = \left[(\tilde{\mathbf{X}}_{-\tilde{m}}^{-1})^T, (\tilde{\mathbf{W}}_{-\tilde{m}}^{-1})^T \right]^T$. The channel input is subject to a time-averaged power constraint \tilde{P} , as in [29, Eq. (7)] and [31, Eq. (7)]:

$$\frac{1}{\tilde{l}} \sum_{i=0}^{\tilde{l}-1} \mathbb{E} \left\{ \left\| \tilde{\mathbf{X}}[i] \right\|^2 \right\} \leq \tilde{P}. \quad (2)$$

Set \tilde{p} to be the least common multiple⁴ of \tilde{p}_G and \tilde{p}_W which satisfies $\tilde{p} > \tilde{m}$. As the CIR and the statistics of the noise of the BB-PLC channel (1) are both periodic with period \tilde{p} , we refer to \tilde{p} as the *period of the channel*. While the above model was stated for real signals, complex (baseband) BB-PLC channels can be accommodated by this model by representing all complex vectors and matrices using real vectors and matrices having twice - for vectors, and four times -

³ Previous works which studied the cyclostationarity of BB-PLC noise, [13], [14], did not explicitly conclude whether the noise process is cyclostationary in the strict-sense or in the wide-sense. We note that in [14, Sec. III-F] it is observed that the marginal PDF of the noise is periodic, which is an indication that the noise process can be modeled as a strict-sense cyclostationary process.

⁴ The common practice in BB-PLC systems, namely, sampling at a rate which is an integer multiple of twice the AC frequency, typically results in $\tilde{p}_G = \tilde{p}_W$ or $\tilde{p}_G = 2\tilde{p}_W$ [13]. In this work we allow a general relationship between the periods of the CIR and of the noise statistics, but still assume synchronized sampling, i.e., we assume that the sampling period is a rational multiple of the period of the continuous-time CIR as well as of the period of the statistics of the continuous-time noise signal. Allowing a general relationship facilitates accommodating additional BB-PLC scenarios, e.g., interference-limited BB-PLC, by our framework.

for matrices, the number of elements, corresponding to the real and to the imaginary parts of the complex components, see, e.g., [32, Sec. I]. Accordingly, a complex MIMO BB-PLC channel with an $\tilde{n}_t^C \times 1$ complex input $\tilde{\mathbf{X}}^C[i]$, an $\tilde{n}_r^C \times 1$ complex output $\tilde{\mathbf{Y}}^C[i]$, an $\tilde{n}_r^C \times 1$ complex additive noise $\tilde{\mathbf{W}}^C[i]$, and an $\tilde{n}_r^C \times \tilde{n}_t^C$ CIR $\{\tilde{\mathbf{G}}^C[i, \tau]\}_{\tau=0}^{\tilde{m}}$, can be equivalently represented as a real MIMO BB-PLC channel corresponding to (1), via the statement in (3).

$$\begin{bmatrix} \text{Re}\{\tilde{\mathbf{Y}}^C[i]\} \\ \text{Im}\{\tilde{\mathbf{Y}}^C[i]\} \end{bmatrix} = \sum_{\tau=0}^{\tilde{m}} \begin{bmatrix} \text{Re}\{\tilde{\mathbf{G}}^C[i, \tau]\} & -\text{Im}\{\tilde{\mathbf{G}}^C[i, \tau]\} \\ \text{Im}\{\tilde{\mathbf{G}}^C[i, \tau]\} & \text{Re}\{\tilde{\mathbf{G}}^C[i, \tau]\} \end{bmatrix} \begin{bmatrix} \text{Re}\{\tilde{\mathbf{X}}^C[i - \tau]\} \\ \text{Im}\{\tilde{\mathbf{X}}^C[i - \tau]\} \end{bmatrix} + \begin{bmatrix} \text{Re}\{\tilde{\mathbf{W}}^C[i]\} \\ \text{Im}\{\tilde{\mathbf{W}}^C[i]\} \end{bmatrix}. \quad (3)$$

In the following section we study the capacity of the MIMO BB-PLC channel defined above subject to a time-averaged power constraint \tilde{P} . The capacity of this channel is denoted as C_{PLC} .

III. THE CAPACITY OF MIMO BB-PLC CHANNELS

Our main result is the characterization of upper and lower bounds on the capacity of MIMO BB-PLC channels, defined in (1). This result is obtained via the following three steps:

- First, in Subsection III-A, we define a general LTI $n_r \times n_t$ MIMO channel with stationary non-Gaussian noise, to which we refer as the *linear non-Gaussian MIMO channel (LNGMC)*. We express the capacity of the LNGMC as a limit of the maximum mutual information between its input and its output as the blocklength increases to infinity.
- Next, we derive computable upper and lower bounds on the capacity of the LNGMC, which are stated in terms of the CIR, and of the entropy rate and autocorrelation of the noise.
- Lastly, in Subsection III-B, we prove that the capacity of the BB-PLC channel can be obtained as the capacity of an equivalent $\tilde{p} \times \tilde{p}$ LNGMC, and use the bounds obtained to state the corresponding capacity bounds for the BB-PLC channel.

A. Analysis of the Capacity of the LNGMC

We begin with the definition of the LNGMC: Let m be a non-negative integer which represents the *length of the memory of the channel*, and let $\{\mathbf{G}[\tau]\}_{\tau=0}^m$ denote a set of $m + 1$ real-valued $n_r \times n_t$ LTI channel transfer matrices. Let $\mathbf{W}[i] \in \mathcal{R}^{n_r}$ be a multivariate, real-valued, strict-sense stationary non-Gaussian additive noise process, whose mean is zero and whose temporal dependence spans a finite interval of length m , i.e., $\forall i_1, i_2, l_1, l_2 \in \mathcal{N}$ such that $i_2 > i_1 + l_1 + m$, the random vectors $\mathbf{W}_{i_1}^{i_1+l_1}$ and $\mathbf{W}_{i_2}^{i_2+l_2}$ are mutually independent. For the transmission of a block of l symbols, the input-output relationship for the channel is given by

$$\mathbf{Y}[i] = \sum_{\tau=0}^m \mathbf{G}[\tau] \mathbf{X}[i - \tau] + \mathbf{W}[i], \quad i \in \{0, 1, \dots, l-1\}, \quad (4)$$

where the initial state of the channel is given by $\mathbf{S}_0 = \left[(\mathbf{X}_{-m}^{-1})^T, (\mathbf{W}_{-m}^{-1})^T \right]^T$. The channel input is subject to a time-averaged power constraint P , i.e.,

$$\frac{1}{l} \sum_{i=0}^{l-1} \mathbb{E} \{ \|\mathbf{X}[i]\|^2 \} \leq P. \quad (5)$$

While the definition of the LNGMC in (4)–(5) can be obtained as a special case of the definition of the MIMO BB-PLC channel in (1)–(2) by setting the period to unity, we use Eqs. (4)–(5) to highlight the fact that the LNGMC is non-periodic and to introduce the different quantities associated with the model separately from the periodic MIMO BB-PLC channel model.

The capacity of the LNGMC defined above is stated in the following proposition:

Proposition 1. *The capacity of the LNGMC defined in (4) subject to (5) is given by*

$$C_L = \lim_{n \rightarrow \infty} \frac{1}{n} \sup_{p(\mathbf{X}^{n-1}): \frac{1}{n} \sum_{i=0}^{n-1} \mathbb{E} \{ \|\mathbf{X}[i]\|^2 \} \leq P} I(\mathbf{X}^{n-1}; \mathbf{Y}^{n-1} | \mathbf{X}_{-m}^{-1} = \mathbf{0}_{n \times m}). \quad (6)$$

Proof: Note that (6) corresponds to the capacity of an *information stable* channel [33]. Information stable channels can be roughly described as having the property that the input which maximizes the mutual information and its corresponding output behave ergodically, thus information stability depends on the conditional PDF of the channel output given the channel input. Since stationary channels with finite memory are known to be information stable⁵, see, e.g., [33, Sec. 1.5], the proposition follows. ■

Comment 1. Previous works on the capacity of finite-memory channels with Gaussian noise, e.g., [31], [36], obtained a capacity result in the frequency domain, by transforming the channel into a set of parallel independent channels, which allows expressing capacity as an explicit integral. When the noise is non-Gaussian, switching to the frequency domain still results in the noise components at different frequency bins having statistical dependence (even if the noise samples are independent in the time domain), and consequently switching to the frequency-domain in such cases will typically not yield a set of parallel independent channels. For this reason, our analysis is carried out in the time domain, and the capacity has to be stated in terms

⁵ The information stability of stationary channels with finite memory, in which the input and the output are taken from *discrete and finite alphabets*, was shown in [34], see also [33, Sec. 1.5]. This results also holds for arbitrary alphabets, see [35, Thm. 6].

of an asymptotic limit. Nonetheless, the *bounds* on the capacity of LNGMCs, derived in Props. 2 and 3, are stated explicitly (not as limit expressions) in the frequency domain.

Prop. 1 implies that the capacity of the LNGMC can be computed by setting $\mathbf{X}_{-m}^{-1} = \mathbf{0}_{n_t \cdot m}$. We note that setting the signal component in the initial state to zero was used as a model assumption in [36] and [37], which studied the capacity of point-to-point channels with memory and Gaussian noise. Note that by defining the $l \cdot n_r \times l \cdot n_t$ matrix $\tilde{\mathbf{G}}_l$ such that

$$\tilde{\mathbf{G}}_l \triangleq \begin{bmatrix} \mathbf{G}[0] & \cdots & 0 & \cdots & 0 \\ \vdots & \ddots & & \ddots & \vdots \\ \mathbf{G}[m] & \cdots & \mathbf{G}[0] & \cdots & 0 \\ \vdots & \ddots & & \ddots & \vdots \\ 0 & \cdots & \mathbf{G}[m] & \cdots & \mathbf{G}[0] \end{bmatrix}, \quad (7)$$

and setting $\mathbf{X}_{-m}^{-1} = \mathbf{0}_{n_t \cdot m}$, the received signal samples can be expressed as

$$\mathbf{Y}^{l-1} = \tilde{\mathbf{G}}_l \mathbf{X}^{l-1} + \mathbf{W}^{l-1}. \quad (8)$$

Next, based on the capacity expression in Prop. 1, we derive upper and lower bounds on C_L , which depend on the distribution of the non-Gaussian noise $\mathbf{W}[i]$ only through its autocorrelation function, $\mathbf{C}_{\mathbf{W}}[\tau] \triangleq \mathbb{E} \left\{ \mathbf{W}[i + \tau] (\mathbf{W}[i])^T \right\}$, and its entropy rate, $\bar{H}_{\mathbf{W}} \triangleq \lim_{l \rightarrow \infty} \frac{1}{l} h(\mathbf{W}^{l-1})$. Note that the strict-sense stationarity and finite temporal dependence of $\mathbf{W}[i]$ imply that the entropy rate limit exists and that it equals $\bar{H}_{\mathbf{W}} = h(\mathbf{W}[m] | \mathbf{W}^{m-1})$ [27, Ch. 12.5].

In the statement of the bounds we make use of the following additional definitions: For any $\omega \in [-\pi, \pi)$, we define the $n_r \times n_t$ matrix $\mathbf{G}'(\omega) \triangleq \sum_{\tau=0}^m \mathbf{G}[\tau] e^{-j\omega\tau}$, and the $n_r \times n_r$ matrix $\mathbf{C}'_{\mathbf{W}}(\omega) \triangleq \sum_{\tau=-m}^m \mathbf{C}_{\mathbf{W}}[\tau] e^{-j\omega\tau}$, and we let $\{\alpha'_k(\omega)\}_{k=0}^{n_r-1}$ and $\{\lambda'_k(\omega)\}_{k=0}^{n_r-1}$ denote the eigenvalues of $\mathbf{G}'(\omega) (\mathbf{G}'(\omega))^H$ and of $(\mathbf{G}'(\omega))^H (\mathbf{C}'_{\mathbf{W}}(\omega))^{-1} \mathbf{G}'(\omega)$, respectively. Next, let $\bar{H}_{G, \mathbf{W}}$ be the entropy rate of a zero-mean $n_r \times 1$ multivariate *Gaussian* process with autocorrelation function $\mathbf{C}_{\mathbf{W}}[\tau]$, and let C_G be the capacity of the channel defined in (4) subject to the constraint (5) and to the setting $\mathbf{X}_{-m}^{-1} = \mathbf{0}_{n_t \cdot m}$, when the noise $\mathbf{W}[i]$ is *Gaussian*. From [38, Sec. III] the entropy rate $\bar{H}_{G, \mathbf{W}}$ can be expressed as

$$\bar{H}_{G, \mathbf{W}} = \frac{1}{4\pi} \int_{\omega=-\pi}^{\pi} \log |2\pi e \mathbf{C}'_{\mathbf{W}}(\omega)| d\omega. \quad (9a)$$

In [37, Eqn. (9)] the capacity of MIMO channels with an LTI CIR and additive stationary

Gaussian noise was characterized⁶, assuming the signal component in the initial state is zero (i.e., $\mathbf{X}_{-m}^{-1} = \mathbf{0}_{n_t \cdot m}$). Using [37, Eqn. (9)] we can write the capacity of the channel (4) when $\mathbf{W}[i]$ is replaced by a zero-mean stationary Gaussian process with the same autocorrelation, as

$$C_G = \frac{1}{4\pi} \sum_{k=0}^{n_r-1} \int_{\omega=-\pi}^{\pi} \left(\log (\Delta' \cdot \lambda'_k(\omega)) \right)^+ d\omega, \quad (9b)$$

where Δ' is selected to satisfy $\frac{1}{2\pi} \sum_{k=0}^{n_r-1} \int_{\omega=-\pi}^{\pi} \left(\Delta' - (\lambda'_k(\omega))^{-1} \right)^+ d\omega = P$.

Note that $\bar{H}_{G,\mathbf{W}}$ and C_G , defined in (9), correspond to the entropy rate of a Gaussian noise process, and to the capacity of a channel with additive Gaussian noise, respectively. These quantities are used for facilitating the characterization of the bounds on the capacity of the LNGMC in which the noise is a non-Gaussian process.

We next state an upper bound and two lower bounds on the capacity of the LNGMC using $\bar{H}_{\mathbf{W}}$, $\bar{H}_{G,\mathbf{W}}$, and C_G . First, the upper bound is stated in the following proposition:

Proposition 2. *The capacity of the LNGMC defined in (4), subject to the constraint (5), satisfies*

$$C_L \leq C_G + \bar{H}_{G,\mathbf{W}} - \bar{H}_{\mathbf{W}}. \quad (10)$$

[A proof is given in Appendix A]

Next, two lower bounds on the capacity of the LNGMC are stated in the following Prop. 3:

Proposition 3. *The capacity of the LNGMC defined in (4) subject to the constraint (5) satisfies*

$$C_L \geq C_G. \quad (11a)$$

Moreover, if $n_r = n_t$ and $\mathbf{G}[0]$ is invertible, then C_L also satisfies

$$C_L \geq \frac{n_r}{2} \log \left(\frac{2\pi e P}{n_t} \cdot 2^{\frac{1}{2\pi \cdot n_t} \sum_{k=0}^{n_r-1} \int_{\omega=-\pi}^{\pi} \log(\alpha'_k(\omega)) d\omega} + 2^{\frac{2}{n_r} \bar{H}_{\mathbf{W}}} \right) - \bar{H}_{\mathbf{W}}. \quad (11b)$$

[A proof is given in Appendix B]

⁶We note that [37, Thm. 1] is stated for a per-codeword power constraint. However, it follows from [37, Sec. 3.1] and from [30, Ch. 7.3, pgs. 323-324] that the proof of [37, Thm. 1] also holds subject to the time-averaged power constraint (5).

B. Capacity Analysis for MIMO BB-PLC Channels

In order to obtain bounds on the capacity of MIMO BB-PLC channels, we first prove that any $\tilde{n}_r \times \tilde{n}_t$ MIMO BB-PLC channel, in which the CIR and the noise statistics are periodic with a period of \tilde{p} , can be equivalently represented (in terms of the achievable rates) as an $\tilde{p} \cdot \tilde{n}_r \times \tilde{p} \cdot \tilde{n}_t$ LNGMC, in which the CIR is time-invariant and the noise is stationary. Then, we apply the capacity bounds derived for the LNGMC to bound the capacity of the original MIMO BB-PLC channel by considering its equivalent LNGMC with the appropriate dimensions. To that aim, define two $\tilde{p} \cdot \tilde{n}_r \times \tilde{p} \cdot \tilde{n}_t$ matrices, $\mathbf{G}_{\text{DCD}}[0]$ and $\mathbf{G}_{\text{DCD}}[1]$, as follows:

$$\mathbf{G}_{\text{DCD}}[0] \triangleq \begin{bmatrix} \tilde{\mathbf{G}}[0,0] & \cdots & 0 & \cdots & 0 \\ \vdots & \ddots & & \ddots & \vdots \\ \tilde{\mathbf{G}}[\tilde{m},\tilde{m}] & \cdots & \tilde{\mathbf{G}}[\tilde{m},0] & \cdots & 0 \\ \vdots & \ddots & & \ddots & \vdots \\ 0 & \cdots & \tilde{\mathbf{G}}[\tilde{p}-1,\tilde{m}] & \cdots & \tilde{\mathbf{G}}[\tilde{p}-1,0] \end{bmatrix}, \quad \mathbf{G}_{\text{DCD}}[1] \triangleq \begin{bmatrix} 0 \cdots 0 & \tilde{\mathbf{G}}[0,\tilde{m}] & \cdots & \tilde{\mathbf{G}}[0,1] \\ \vdots & \vdots & & \ddots & \vdots \\ 0 \cdots 0 & 0 & & \tilde{\mathbf{G}}[\tilde{m}-1,\tilde{m}] \\ \vdots & \vdots & \vdots & & \vdots \\ 0 \cdots 0 & 0 & \cdots & 0 \end{bmatrix},$$

and also define the $\tilde{p} \cdot \tilde{n}_r \times 1$ random vector $\mathbf{W}_{\text{DCD}}[\tilde{i}] \triangleq \tilde{\mathbf{W}}_{\tilde{i}\tilde{p}}^{(\tilde{i}+1)\cdot\tilde{p}-1}$. As $\mathbf{W}_{\text{DCD}}[\tilde{i}]$ is given by the decimated components decomposition (DCD) [42] of $\tilde{\mathbf{W}}[\tilde{i}]$, the strict-sense cyclostationarity of $\tilde{\mathbf{W}}[\tilde{i}]$ induces a strict-sense stationarity of $\mathbf{W}_{\text{DCD}}[\tilde{i}]$. Using these definitions, we construct an LNGMC with a $\tilde{p} \cdot \tilde{n}_t \times 1$ input $\mathbf{X}_{\text{DCD}}[\tilde{i}]$ and a $\tilde{p} \cdot \tilde{n}_r \times 1$ output $\mathbf{Y}_{\text{DCD}}[\tilde{i}]$ which satisfies the following input-output relationship for a sequence of l channel inputs:

$$\mathbf{Y}_{\text{DCD}}[\tilde{i}] = \sum_{\tilde{\tau}=0}^1 \mathbf{G}_{\text{DCD}}[\tilde{\tau}] \mathbf{X}_{\text{DCD}}[\tilde{i}-\tilde{\tau}] + \mathbf{W}_{\text{DCD}}[\tilde{i}], \quad \tilde{i} \in \{0, 1, \dots, l-1\}, \quad (12)$$

where the channel input to the LNGMC (12) has to satisfy an average power constraint

$$\frac{1}{l} \sum_{\tilde{i}=0}^{l-1} \mathbb{E} \left\{ \|\mathbf{X}_{\text{DCD}}[\tilde{i}]\|^2 \right\} \leq P_{\text{DCD}} = \tilde{p} \cdot \tilde{P}. \quad (13)$$

Since $\tilde{p} > \tilde{m}$, the initial state of the LNGMC is $\mathbf{S}_{0,\text{DCD}} = [\mathbf{X}_{\text{DCD}}^T[-1], \mathbf{W}_{\text{DCD}}^T[-1]]^T$. Let C_{DCD} be the capacity of the LNGMC defined in (12)–(13). The relationship between the capacity of the BB-PLC channel in (1)–(2) and the LNGMC in (12)–(13) is stated in the following theorem:

Theorem 1. *The capacity of the BB-PLC channel, defined in (1), subject to (2) satisfies*

$$C_{\text{PLC}} = \frac{1}{\tilde{p}} C_{\text{DCD}}. \quad (14)$$

[A proof is given in Appendix C]

Based on Thm. 1 and Props. 2 and 3, we obtain lower and upper bounds on the capacity of the BB-PLC channel. To that aim, define the $\tilde{p} \cdot \tilde{n}_r \times \tilde{p} \cdot \tilde{n}_r$ autocorrelation function $\mathbf{C}_{\mathbf{W}_{\text{DCD}}}[\tilde{\tau}] \triangleq \mathbb{E} \{ \mathbf{W}_{\text{DCD}}[\tilde{i} + \tilde{\tau}] \mathbf{W}_{\text{DCD}}^T[\tilde{i}] \}$, the entropy rate $\bar{H}_{\mathbf{W}_{\text{DCD}}} \triangleq \lim_{n \rightarrow \infty} \frac{1}{n} h(\mathbf{W}_{\text{DCD}}^{n-1})$, the $\tilde{p} \cdot \tilde{n}_r \times \tilde{p} \cdot \tilde{n}_r$ matrix $\mathbf{G}'_{\text{DCD}}(\omega) \triangleq \sum_{\tilde{\tau}=0}^1 \mathbf{G}_{\text{DCD}}[\tilde{\tau}] e^{-j\omega\tilde{\tau}}$, and the $\tilde{p} \cdot \tilde{n}_r \times \tilde{p} \cdot \tilde{n}_r$ matrix $\mathbf{C}'_{\mathbf{W}_{\text{DCD}}}(\omega) \triangleq \sum_{\tilde{\tau}=-1}^1 \mathbf{C}_{\mathbf{W}_{\text{DCD}}}[\tilde{\tau}] e^{-j\omega\tilde{\tau}}$. Next, let $\{\alpha'_{\text{DCD},k}(\omega)\}_{k=0}^{\tilde{p} \cdot \tilde{n}_r - 1}$ and $\{\lambda'_{\text{DCD},k}(\omega)\}_{k=0}^{\tilde{p} \cdot \tilde{n}_r - 1}$ be the eigenvalues of $\mathbf{G}'_{\text{DCD}}(\omega)$ ($\mathbf{G}'_{\text{DCD}}(\omega)$)^H and of $(\mathbf{G}'_{\text{DCD}}(\omega))^H (\mathbf{C}'_{\mathbf{W}_{\text{DCD}}}(\omega))^{-1} \mathbf{G}'_{\text{DCD}}(\omega)$, respectively, and, in addition, let $\bar{H}_{G, \mathbf{W}_{\text{DCD}}}$ denote the entropy rate of a zero mean $\tilde{p} \cdot \tilde{n}_r \times 1$ Gaussian process with autocorrelation function $\mathbf{C}_{\mathbf{W}_{\text{DCD}}}[\tilde{\tau}]$. $\bar{H}_{G, \mathbf{W}_{\text{DCD}}}$ can be computed via (9a) with $\mathbf{C}'_{\mathbf{W}_{\text{DCD}}}(\omega)$ instead of $\mathbf{C}'_{\mathbf{W}}(\omega)$. Finally, let $C_{\text{DCD},G}$ be the capacity of the LNGMC (12) when the noise $\mathbf{W}_{\text{DCD}}[\tilde{i}]$ is Gaussian with autocorrelation function $\mathbf{C}_{\mathbf{W}_{\text{DCD}}}[\tilde{\tau}]$. Thus, $C_{\text{DCD},G}$ is obtained using (9b) with $\lambda'_{\text{DCD},k}(\omega)$ and P_{DCD} replacing $\lambda'_k(\omega)$ and P , respectively. Noting that $\mathbf{G}_{\text{DCD}}[0]$ has a full rank if and only if $\tilde{\mathbf{G}}[\tilde{i}, 0]$ has a full rank for every $\tilde{i} \in \{0, 1, \dots, \tilde{p} - 1\} \triangleq \tilde{\mathcal{P}}$ [51, Ex. 3.7.4], then, by combining Thm. 1 with Prop. 2, the following upper bound on C_{PLC} is obtained:

Corollary 1. *The capacity of the BB-PLC channel defined in (1), subject to (2), satisfies*

$$C_{\text{PLC}} \leq \frac{1}{\tilde{p}} (C_{\text{DCD},G} + \bar{H}_{G, \mathbf{W}_{\text{DCD}}} - \bar{H}_{\mathbf{W}_{\text{DCD}}}). \quad (15)$$

Lastly, combining Thm. 1 with Prop. 3, the following lower bounds on C_{PLC} are obtained:

Corollary 2. *The capacity of the BB-PLC channel defined in (1), subject to (2), satisfies*

$$C_{\text{PLC}} \geq \frac{1}{\tilde{p}} C_{\text{DCD},G}. \quad (16a)$$

Moreover, if $\tilde{n}_r = \tilde{n}_t$ and $\tilde{\mathbf{G}}[\tilde{i}, 0]$ is non-singular for every $\tilde{i} \in \tilde{\mathcal{P}}$, then C_{PLC} also satisfies

$$C_{\text{PLC}} \geq \frac{\tilde{n}_t}{2} \log \left(\frac{2\pi e \tilde{P}}{\tilde{n}_t} \cdot 2^{\frac{1}{2\pi \cdot \tilde{p} \cdot \tilde{n}_t}} \sum_{k=0}^{\tilde{p} \cdot \tilde{n}_r - 1} \int_{\omega=-\pi}^{\pi} \log(\alpha'_{\text{DCD},k}(\omega)) d\omega + 2^{\frac{2}{\tilde{p} \cdot \tilde{n}_r}} \bar{H}_{\mathbf{W}_{\text{DCD}}} \right) - \frac{1}{\tilde{p}} \bar{H}_{\mathbf{W}_{\text{DCD}}}. \quad (16b)$$

Comment 2. From the proof of Prop. 3 in Appendix B we note that the lower bounds (11b) in Prop. 3 also lower bound the achievable rate of the LNGMC with *stationary multivariate Gaussian input*. This implies that (16b) constitutes a lower bound on the achievable rate of BB-PLC channels with cyclostationary Gaussian input. Consequently, when (16b) coincides with the upper bound in (15), then cyclostationary Gaussian inputs are optimal.

IV. APPLICATION: CAPACITY BOUNDS FOR SEVERAL BB-PLC CHANNEL MODELS

The capacity bounds derived in Section III depend on the marginal distribution of the noise in the BB-PLC channel, $\tilde{\mathbf{W}}[i]$, only through its entropy rate. In this section we derive explicit expressions for the entropy rates of two common non-Gaussian BB-PLC noise models: The Nakagami- m model [4], and the GM⁷ model [8]. We first consider the case in which the noise is an i.i.d. process, and thus its entropy rate is equal to the differential entropy of a single sample [27, Ch. 4.2]. In such cases, the entropy rate of the noise process can be computed using only the marginal distribution of the noise. When the noise is correlated, then the derivation of the entropy rate requires the characterization of the complete statistics of the noise process, which is typically unavailable for the current BB-PLC channel models. Thus, in this work we incorporate periodically time varying noise autocorrelation functions by applying LPTV filtering to an i.i.d. noise process, and using the entropy rate of the resulting output process in our expressions. In order to apply this approach, we first derive a relationship between the entropy rates at the input and at the output of LPTV filters, when the input is an i.i.d. process. We note, however, that for non-Gaussian processes, LPTV filtering typically does not preserve the marginal distribution of the input process at the output, hence the resulting output process will typically have a mismatched marginal distribution w.r.t. that of the input process. Accordingly, the bounds obtained using the proposed approach should be considered as an indication of the bounds on the capacity of BB-PLC channels with correlated noise. In the following we propose exact expressions and bounds on the entropy rate $\bar{H}_{\mathbf{W}_{\text{DCD}}}$. These expressions and bounds can be used in Corollaries 1 and 2 to obtain bounds on the capacity of several BB-PLC models.

A. *i.i.d. Complex Nakagami- m Noise*

The complex Nakagami- m noise model is a model for the additive noise in baseband BB-PLC channels [4], accommodated by our real multivariate model (1) by representing complex signals using real multivariate signals. To facilitate the introduction of this noise model, we recall the definition of the real-valued Nakagami- m distribution:

Definition 5 (Real-valued Nakagami- m distribution). *A real-valued scalar RV is said to follow a Nakagami- m distribution with shape parameter $m \geq \frac{1}{2}$ and second-order moment $\Omega > 0$ if its PDF is given by [53, Ch. 4.18]*

⁷The Middleton class A distribution, which is another important BB-PLC noise model, can be approximated using a GM distribution [8], thus the entropy rate of a Middleton class A noise can be approximated using the entropy rate of a GM process.

$$f_X(x) = \frac{2}{\Gamma(m)} \left(\frac{m}{\Omega}\right)^m x^{2m-1} e^{-\frac{mx^2}{\Omega}}, \quad x \geq 0, \quad (17)$$

where $\Gamma(\cdot)$ denotes the Gamma function. We denote this distribution with $X \sim \mathcal{KG}(m, \Omega)$.

The real-valued Nakagami- m distribution is commonly used to model the distribution of the *amplitude* of the noise in baseband BB-PLC channels [4]–[6], for which the marginal distribution of the baseband noise is a complex-valued Nakagami- m PDF [4], defined as follows:

Definition 6 (Complex-valued Nakagami- m distribution [4]). *Let $X \sim \mathcal{KG}(m, \Omega)$, and let Θ be an RV uniformly distributed over $[0, 2\pi]$, mutually independent of X . Then, $W = Xe^{j\Theta}$ is a complex Nakagami- m RV with zero mean and variance Ω , and is denoted by $W \sim \mathcal{CKG}(m, \Omega)$.*

Letting $\Psi(\cdot)$ denote the Digamma function [53, Tbl. 0.1], the differential entropy of a complex Nakagami- m RV is stated in the following proposition:

Proposition 4. *The differential entropy of $W \sim \mathcal{CKG}(m, \Omega)$ is given by:*

$$h(W) = \frac{1}{2\ln(2)}\Psi(m) + \log\left(\frac{\pi\Omega}{m}\Gamma(m)e^{\frac{2m-(2m-1)\Psi(m)}{2}}\right) \quad (18)$$

[A proof is given in Appendix D]

Now, for scalar BB-PLC channels in which the noise is modeled as an i.i.d. complex Nakagami- m process, the entropy rate $\bar{H}_{\mathbf{W}_{\text{DCD}}}$ is given by (18), which can be used in (15)-(16) to obtain upper and lower bounds on the capacity.

B. i.i.d. Gaussian Mixture Noise

Next, we consider an additive multivariate real-valued GM noise, which is another common model for BB-PLC noise, see, e.g., [8]. This model is again obtained by representing the complex-valued baseband channel as a real-valued channel of extended dimensions.

Let $f_{G_{\tilde{n}_r}}(\mathbf{u}; \mathbf{m}, \mathbf{C})$ denote the PDF of an $\tilde{n}_r \times 1$ real Gaussian random vector with mean vector $\mathbf{m} \in \mathcal{R}^{\tilde{n}_r}$ and covariance matrix $\mathbf{C} \in \mathcal{R}^{\tilde{n}_r \times \tilde{n}_r}$, where \mathbf{u} denotes the realization of the random vector, i.e., $f_{G_{\tilde{n}_r}}(\mathbf{u}; \mathbf{m}, \mathbf{C}) = |2\pi\mathbf{C}|^{-1/2}e^{-(\mathbf{u}-\mathbf{m})^T\mathbf{C}^{-1}(\mathbf{u}-\mathbf{m})}$. The distribution of a GM random vector $\mathbf{W} \in \mathcal{R}^{\tilde{n}_r}$ is determined by the number of Gaussians n_G , $n_G \geq 1$, the set of positive mixing parameters $\{\gamma_n\}_{n=1}^{n_G}$ satisfying $\sum_{n=1}^{n_G} \gamma_n = 1$, the set of mean vectors $\{\mathbf{m}_n\}_{n=1}^{n_G}$, and the set of covariances matrices $\{\mathbf{C}_n\}_{n=1}^{n_G}$. Using these parameters, the PDF of \mathbf{W} is given by:

$$f_{\mathbf{W}}(\mathbf{w}) = \sum_{n=1}^{n_G} \gamma_n \cdot f_{G_{\tilde{n}_r}}(\mathbf{w}; \mathbf{m}_n, \mathbf{C}_n). \quad (19)$$

While there is no closed-form analytic expression for the differential entropy of GM random vectors [50], upper and lower bounds on the differential entropy of GM random vectors can be obtained as stated in [50, Thm. 2-3], repeated here for convenience:

Theorem. [50, Thms. 2-3]. *The differential entropy of a random vector with PDF (19) satisfies*

$$-\sum_{n=1}^{n_G} \gamma_n \cdot \log \left(\sum_{m=1}^{n_G} \gamma_m \cdot f_{G_{\tilde{n}_r}}(\mathbf{m}_n; \mathbf{m}_m, C_m + C_n) \right) \leq h(\mathbf{W}) \leq \sum_{n=1}^{n_G} \gamma_n \cdot \left(\frac{1}{2} \log |2\pi e C_n| - \log(\gamma_n) \right).$$

The bounds in [50, Thms. 2-3] are tight when the number of Gaussian components is small⁸ and when the Gaussians are well separated from each other [50], which applies to the GM BB-PLC noise model in [8]. As for i.i.d. noise $\bar{H}_{\mathbf{W}_{\text{DCD}}} = h(\mathbf{W})$, [50, Thms. 2-3] provide tight bounds on the entropy rate of i.i.d. GM noise for small n_G and sufficiently separated Gaussians.

C. Correlated Non-Gaussian Cyclostationary Noise

In the previous subsections we studied the differential entropy of two i.i.d. BB-PLC noise models. As in many BB-PLC systems the noise process is modeled as a temporally correlated [8]–[12] cyclostationary process [9], [13], [14], we propose an approach for extending the derivation of the differential entropy for i.i.d. noise models studied in Subsections IV-A–IV-B to correlated non-Gaussian cyclostationary noise models.

In order to compute the capacity bounds in (15)-(16), it is required to compute $\frac{1}{p} \bar{H}_{\mathbf{W}_{\text{DCD}}}$, which is the entropy rate of the multivariate noise process $\mathbf{W}_{\text{DCD}}[\tilde{i}]$. As the noise $\tilde{\mathbf{W}}[i]$ is a temporally and spatially correlated non-Gaussian cyclostationary process, then computing the entropy rate of $\mathbf{W}_{\text{DCD}}[\tilde{i}]$ requires the complete statistics of the noise process. We note, however, that complete statistical models for the noise in BB-PLC channels are currently not available for most typical BB-PLC scenarios [8]. In the following we apply the widely acceptable practice of generating a correlated noise process via filtering an appropriate i.i.d. process. Accordingly, we propose to obtain an explicit expression for the entropy rate by modeling the noise process as the output of an LPTV filter with an i.i.d. non-Gaussian input. This model accounts for the non-Gaussianity of the noise, as well as for its cyclostationarity, temporal correlation, and spatial correlation. We note that the approach has been applied previously in the context of noise generation for narrowband PLC systems in [46], [47]. The noise signal is generated as described below: First, we let $\tilde{\mathbf{U}}[i] \in \mathcal{R}^{\tilde{n}_r}$ be an i.i.d. random process, and let $\{\tilde{F}[i, \tau]\}_{\tau=0}^{\tilde{m}}$ be the CIR of

⁸In the case of $n_G = 1$, i.e., a multivariate Gaussian distribution, the upper bound is the differential entropy.

an $\tilde{n}_r \times \tilde{n}_r$ LPTV filter with period \tilde{p} and memory \tilde{m} , where $\tilde{F}[i, 0]$ is non-singular $\forall i \in \tilde{\mathcal{P}}$. The noise process is then generated via

$$\tilde{\mathbf{W}}[i] = \sum_{\tau=0}^{\tilde{m}} \tilde{F}[i, \tau] \tilde{\mathbf{U}}[i - \tau]. \quad (20)$$

Note that the resulting noise process $\tilde{\mathbf{W}}[i]$ is a strict-sense cyclostationary process with a period of \tilde{p} samples and a temporal correlation which spans an interval of \tilde{m} samples, hence it satisfies the model assumptions in Subsection II-C.

We next consider blocks of $\tilde{p} \cdot \tilde{n}_r$ samples of $\tilde{\mathbf{W}}[i]$, and restate the LPTV filtering of (20) as a multivariate LTI filtering of extended dimensions. To that aim, define the $\tilde{p} \cdot \tilde{n}_r \times \tilde{p} \cdot \tilde{n}_r$ matrices $\mathbf{F}[0]$ and $\mathbf{F}[1]$:

$$\mathbf{F}[0] \triangleq \begin{bmatrix} \tilde{F}[0, 0] & \cdots & 0 & \cdots & 0 \\ \vdots & \ddots & & \ddots & \vdots \\ \tilde{F}[\tilde{m}, \tilde{m}] & \cdots & \tilde{F}[\tilde{m}, 0] & \cdots & 0 \\ \vdots & \ddots & & \ddots & \vdots \\ 0 & \cdots & \tilde{F}[\tilde{p}-1, \tilde{m}] & \cdots & \tilde{F}[\tilde{p}-1, 0] \end{bmatrix}, \quad \mathbf{F}[1] \triangleq \begin{bmatrix} 0 \cdots 0 & \tilde{F}[0, \tilde{m}] \cdots & \tilde{F}[0, 1] \\ \vdots & \vdots & \ddots & \vdots \\ 0 \cdots 0 & 0 & \tilde{F}[\tilde{m}-1, \tilde{m}] \\ \vdots & \vdots & \vdots & \vdots \\ 0 \cdots 0 & 0 & \cdots & 0 \end{bmatrix},$$

and let $\mathbf{F}'(\omega) \triangleq \sum_{\tau=0}^1 \mathbf{F}[\tau] e^{-j\omega\tau}$. Also, recall that $\mathbf{W}_{\text{DCD}}[\tilde{i}] \triangleq \tilde{\mathbf{W}}_{\tilde{i}, \tilde{p}}^{(\tilde{i}+1) \cdot \tilde{p}-1}$ and let $\mathbf{U}[\tilde{i}] \triangleq \tilde{\mathbf{U}}_{\tilde{i}, \tilde{p}}^{(\tilde{i}+1) \cdot \tilde{p}-1}$. From (20) we obtain the following relationship between $\mathbf{W}_{\text{DCD}}[\tilde{i}]$ and $\mathbf{U}[\tilde{i}]$:

$$\mathbf{W}_{\text{DCD}}[\tilde{i}] = \sum_{\tilde{\tau}=0}^1 \mathbf{F}[\tilde{\tau}] \mathbf{U}[\tilde{i} - \tilde{\tau}]. \quad (21)$$

Since $\tilde{\mathbf{U}}[i]$ is an i.i.d. process, it follows that the entropy rate of $\mathbf{U}[\tilde{i}]$ is given by $\tilde{p} \cdot h(\tilde{\mathbf{U}})$. We can now obtain the time-averaged entropy rate of $\mathbf{W}_{\text{DCD}}[\tilde{i}]$ as stated in the following lemma:

Lemma 1. *The time-average of the entropy rate of $\mathbf{W}_{\text{DCD}}[\tilde{i}]$ is given by*

$$\frac{1}{\tilde{p}} \bar{H}_{\mathbf{W}_{\text{DCD}}} = \frac{1}{2\pi \cdot \tilde{p}} \int_{\omega=0}^{2\pi} \log |\mathbf{F}'(\omega)| d\omega + h(\tilde{\mathbf{U}}). \quad (22)$$

[A proof is given in Appendix E]

We note that modeling the noise via (20) allows us to evaluate the entropy rate for non-Gaussian, temporally correlated, and cyclostationary BB-PLC noise models. It should be noted that, in general, the marginal distribution of $\tilde{\mathbf{W}}[i]$ may be different than the marginal distribution

of the i.i.d. signal $\tilde{\mathbf{U}}[i]$, e.g., when $\tilde{\mathbf{U}}[i]$ follows a complex Nakagami- m distribution, yet, when $\tilde{\mathbf{U}}[i]$ is a GM process, then the filtered process in (20) is also a GM process, but the number of Gaussians and their parameters may change [43].

V. NUMERICAL EXAMPLES AND DISCUSSION

In this section we numerically evaluate the capacity bounds derived in Section III for various BB-PLC channels. The simulation study consists of two parts: First, in Subsection V-A we illustrate the effect of the non-Gaussianity of the noise on the capacity of the channel. Then, in Subsection V-B we evaluate the capacity bounds for some BB-PLC channel models, considering both scalar as well as MIMO models, and discuss the tightness of these bounds.

To compute the capacity bounds for the GM noise, we first compute upper and lower bounds on the differential entropy $\bar{H}_{\mathbf{W}_{\text{DCD}}}$, denoted $\bar{H}_{\mathbf{W}_{\text{DCD}}}^{(\text{up.})}$ and $\bar{H}_{\mathbf{W}_{\text{DCD}}}^{(\text{low.})}$, respectively, as detailed in Subsection IV-B. Then, we compute the upper bound in (15) by replacing $\frac{1}{p}\bar{H}_{\mathbf{W}_{\text{DCD}}}$ with $\frac{1}{p}\bar{H}_{\mathbf{W}_{\text{DCD}}}^{(\text{low.})}$, and the lower bound in (16b) (denoted *Lower bound 2*) is computed with $\frac{1}{p}\bar{H}_{\mathbf{W}_{\text{DCD}}}$ replaced with⁹ $\frac{1}{p}\bar{H}_{\mathbf{W}_{\text{DCD}}}^{(\text{up.})}$. Lastly, we note that the lower bound in (16a) (denoted *Lower bound 1*) does not depend on the entropy rate. As BB-PLC channels exhibit a broad range of signal attenuation and noise power values, depending on the topology of the power line network and on the appliances connected to the network [4], [9], [10], [13], we consider a wide range of SNR values.

A. Evaluating the Effect of the non-Gaussianity of the Noise

As noted in Section I, previous works on the fundamental rate limits of BB-PLC channels, e.g., [7], [10], [26], assumed that the additive noise is Gaussian, which facilitated obtaining an explicit expression for the capacity. Nonetheless, BB-PLC noise is typically modeled as a *non-Gaussian process*, and two common models for its marginal PDF are the Nakagami- m distribution [4] and the GM distribution [8]. In the following we illustrate the effect of the non-Gaussianity of the additive BB-PLC noise on the capacity of the channel, and numerically evaluate the mismatch induced by assuming that the noise is Gaussian (e.g., as done in some previous works, including [10], [26]) compared to the actual capacity. To that aim, we consider a memoryless ($\tilde{m} = 1$), time-invariant ($\tilde{p} = 1$), scalar baseband channel, in which the additive noise $\tilde{W}[i]$ is an i.i.d. process. We consider two marginal distributions of the noise: The first noise process

⁹Since for $a, b > 0$, the function $f(x) = a \cdot \log(b + 2^{x/a}) - x$ is monotonically non-decreasing w.r.t. x , then, computing (16b) with $\frac{1}{p}\bar{H}_{\mathbf{W}_{\text{DCD}}}^{(\text{low.})}$ instead of $\frac{1}{p}\bar{H}_{\mathbf{W}_{\text{DCD}}}$ results in a lower bound on the capacity.

follows a complex GM distribution. In this case, in order to generate $\tilde{W}[i]$, we let $\tilde{Z}[i]$ be an i.i.d. complex process such that $[\text{Re}\{\tilde{Z}[i]\}, \text{Im}\{\tilde{Z}[i]\}]^T$ is a 2×1 GM random vector with parameters $n_G = 3$, $\{\gamma_n\}_{n=1}^3 = \{0.7, 0.2, 0.1\}$, $\{\mathbf{m}_n\}_{n=1}^3 = \{[5, 4]^T, [-8, -16]^T, [-19, 4]^T\}$, and $\{\mathbf{C}_n\}_{n=1}^3 = \{5, 2, 1\} \cdot \mathbf{I}_2$, following [8, Fig. 3a]. Then, we set $\alpha = \mathbb{E}\{|\tilde{Z}[i]|^2\}^{-1/2}$, and obtain the noise as $\tilde{W}[i] = \alpha \cdot \tilde{Z}[i]$; We also consider noise with a complex Nakagami- m distribution with parameters $m = 0.8$ and $\Omega = 1$, as in [4]. Note that both noise models have a zero mean and a unit variance. This scenario accounts only for the non-Gaussianity of the noise in the channel model, and neglects the effects of the channel memory and of the non-stationarity of the noise.

Fig. 1 depicts the capacity bounds for this scenario vs. SNR, defined here as $\text{SNR} = \frac{\tilde{P}}{\mathbb{E}\{|\tilde{W}[i]|^2\}}$. Note that the lower bound in (16a) (*Lower bound 1* in Fig. 1), which represents the capacity of the channel assuming that the noise is Gaussian, does not depend on the actual distribution of the noise, and is therefore the same for both simulated noise distributions. Observing Fig. 1, we note that for GM noise, there is a substantial gap between the actual capacity of the channel and the capacity computed assuming that the noise is Gaussian, especially in high SNR. For example, at SNR of 12 dB, capacity is not less than 7 bps/Hz, while assuming Gaussian noise, the SNR has to be increased by at least 9 dB in order to obtain the same capacity of 7 bps/Hz. A less notable gap is observed for Nakagami- m noise, where an SNR gap of 0.7 dB is observed for capacity of 7 bps/Hz. Moreover, we note that for the Nakagami- m noise, the lower bound in (16b) numerically coincides with the upper bound for SNRs greater than 10 dB. As discussed in Comment 2, this implies that Gaussian inputs are *optimal* at high SNR for the Nakagami- m noise channel. For the GM noise model, we observe a gap of 0.5 bps/Hz between the lower bound (16b) and the upper bound (15), for SNRs above 10 dB. Consequently, as (16b) lower bounds the achievable rate with Gaussian inputs, we conclude that for the GM noise model, the achievable rate of Gaussian inputs is at most 0.5 bps/Hz less than capacity at high SNR.

B. Capacity of BB-PLC Channels with Correlated Non-Gaussian Noise

We now use the results in Corollaries 1 and 2 to characterize bounds on the capacity of practical BB-PLC channel models. The channel models considered here are taken from the recent literature on BB-PLC channel modeling, and are selected to represent actual BB-PLC channels. We first study the capacity of the scalar passband BB-PLC scenario: The LPTV CIR is generated

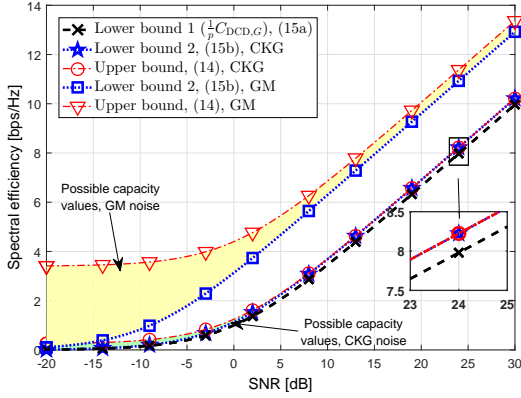


Fig. 1. Capacity bounds for the i.i.d. noise channel, with complex Nakagami- m (CKG) and GM noise models.

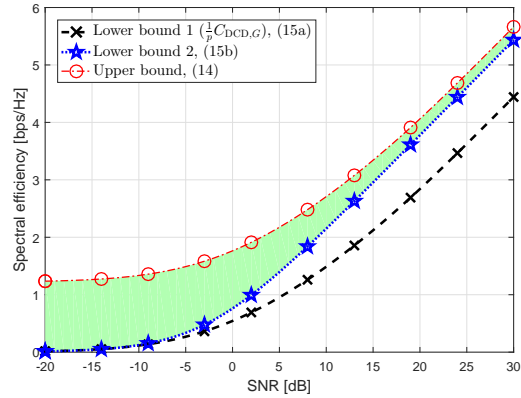


Fig. 2. Capacity bounds for the scalar BB-PLC channel, with the **GM1** noise model.

with period a $\tilde{p}_G = 240$ and memory length¹⁰ $\tilde{m} = 4$ using the channel generator proposed in [19], where the parameters used by the channel generator were set to the default values. The additive noise is a non-Gaussian temporally correlated cyclostationary process, generated using the approach described in Subsection IV-C: First, an i.i.d. scalar process $\tilde{U}[i]$ is generated, where we consider three PDFs for $\tilde{U}[i]$:

- **GM1** - a GM PDF based on [8, Fig. 3a] with parameters $n_G = 3$, $\{\gamma_n\}_{n=1}^3 = \{0.7, 0.2, 0.1\}$, $\{m_n\}_{n=1}^3 = \{5, -8, -19\}$, and $\{c_n\}_{n=1}^3 = \{5, 2, 1\}$;
- **GM2** - a GM PDF based on [40, Fig. 2] with parameters $n_G = 3$, $\{\gamma_n\}_{n=1}^3 = \{0.9, 0.07, 0.03\}$, $\{m_n\}_{n=1}^3 = \{0, 0, 0\}$, and $\{c_n\}_{n=1}^3 = \{1, 100, 1000\}$;
- **MCA** - a GM PDF approximating a Middleton Class A PDF as in [41, Ch. 2.7.2] with parameters based on [40, Fig. 3], i.e., letting $A = 0.1$ and $\Omega = 0.01$, and setting $n_G = 10$, $\gamma_n = e^{-A \frac{A^n}{n!}}$, $m_n = 0$, and $c_n = \frac{n/A + \Omega}{1 + \Omega}$, $n \in \{0, 1, \dots, n_G - 1\}$.

The process $\tilde{U}[i]$ is normalized to have a unit variance, and is then filtered via a spectral shaping LPTV filter to obtain the scalar BB-PLC noise $\tilde{W}[i]$. Two spectral shaping LPTV filters with period $\tilde{p}_W = 120$ and memory length $\tilde{m} = 4$ are used: The first is a filter designed to generate the periodically time-varying BB-PLC ‘*medium disturbed*’ correlation profile. This filter is applied to the **GM1** and **GM2** noise signals. The second spectral shaping filter is designed to generate the periodically time-varying BB-PLC ‘*heavily disturbed*’ correlation profile, and is applied to the **MCA** noise model. Both correlation profiles were obtained from actual BB-PLC noise

¹⁰Note that the root mean-square (RMS) delay spread in BB-PLC channels is typically on the order of several microseconds, i.e., around 0.1% of the channel period [3, Tbl. 1]. Thus, following the typical relationship between RMS delay spread and memory length, see, e.g., [39, Ch. 3.3.1], the memory length is on the order of 1% of the channel period.

measurements via the procedure detailed in [14]¹¹. Note that for the values selected for \tilde{p}_G and \tilde{p}_W , then \tilde{p} , which is the least common multiple of \tilde{p}_G and \tilde{p}_W not smaller than \tilde{m} , equals $\tilde{p} = 240$.

The capacity bounds for the scalar BB-PLC channel vs. SNR, defined here as $\text{SNR} = \frac{\tilde{P}}{\frac{1}{\tilde{p}} \sum_{i=1}^{\tilde{p}} \mathbb{E}\{|\tilde{W}[i]|^2\}}$, are depicted in Figs. 2-4, for the **GM1** noise, **GM2** noise, and **MCA** noise, respectively. Observing Figs. 2-4, we note that the lower bound in (16b) (*Lower bound 2* in Figs. 2-4) is much tighter than the lower bound in (16a) (*Lower bound 1* in Figs. 2-4) for all the noise models considered. Consequently, assuming that the *noise is Gaussian* results in a capacity expression which is *strictly smaller* than the actual capacity, and for most SNR values, this expression is considerably less than the actual capacity. It thus follows that using the Gaussian noise assumption leads to schemes whose achievable rates are far from achieving the maximal bit rate that can be supported by the BB-PLC channel. Additionally, we note that for SNRs higher than 10 dB, the lower bound (16b) is lower than the upper bound (15) by only 0.25 bps/Hz, 0.8 bps/Hz, and 0.6 bps/Hz, for the the **GM1** noise, the **GM2** noise, and the **MCA** noise, respectively. We conclude that, for the tested scenarios at high SNRs, the bounds in (16b) and (15) are relatively tight, hence Corollaries 1 and 2 provide a reliable characterization of the capacity. We also conclude that at high SNRs the achievable rate obtained with cyclostationary Gaussian inputs is within a small gap from capacity.

Next, we consider a passband 2×2 MIMO BB-PLC scenario. The multivariate LPTV CIR $\tilde{\mathbf{G}}[i, \tau]$ was generated using the method proposed in [22] for generating MIMO BB-PLC channels based on the characteristics of the scalar channel. Specifically, we first generate four real LPTV CIRs with period $\tilde{p}_G = 240$ and memory length $\tilde{m} = 4$ using the channel generator proposed in [19]. We denote the generated channels as $\{\tilde{g}_k[i, \tau]\}_{k=1}^4$. Then, setting $\rho = 0.9$ [22, Sec. V-B], the multivariate LPTV CIR is obtained via

$$\tilde{\mathbf{G}}[i, \tau] = \begin{bmatrix} 1 & \rho \\ \rho & 1 \end{bmatrix}^{1/2} \begin{bmatrix} \tilde{g}_1[i, \tau] & \tilde{g}_2[i, \tau] \\ \tilde{g}_3[i, \tau] & \tilde{g}_4[i, \tau] \end{bmatrix} \begin{bmatrix} 1 & \rho \\ \rho & 1 \end{bmatrix}^{1/2}.$$

The additive multivariate noise $\tilde{\mathbf{W}}[i]$ is generated using the model detailed in Subsection IV-C: First, a real i.i.d. 2×1 process $\tilde{\mathbf{U}}[i]$ is generated, normalized to having a unit variance. We used

¹¹The ‘medium disturbed’ and ‘heavily disturbed’ correlation profiles obtained following [14] are available on <http://www.plc.uma.es/channels.htm>.

two different PDFs for $\tilde{\mathbf{U}}[i]$:

- **MIMO GM** - a GM PDF based on [8, Fig. 3a] with parameters $n_G = 3$, $\{\gamma_n\}_{n=1}^3 = \{0.7, 0.2, 0.1\}$, $\{\mathbf{m}_n\}_{n=1}^3 = \{[5, 4]^T, [-8, -16]^T, [-19, 4]^T\}$, and $\{\mathbf{C}_n\}_{n=1}^3 = \{5, 2, 1\} \cdot \mathbf{I}_2$.
- **MIMO MCA** - a GM PDF approximating a Middleton Class A PDF as in [41, Ch. 2.7.2] with parameters based on [40, Fig. 3], i.e., letting $A = 0.1$ and $\Omega = 0.01$, such that $n_G = 10$, $\gamma_n = e^{-A \frac{A^n}{n!}}$, $\mathbf{m}_n = [0, 0]^T$, and $\mathbf{C}_n = \frac{n/A+\Omega}{1+\Omega} \cdot \mathbf{I}_2$, $n \in \{0, 1, \dots, n_G - 1\}$.

Next, we generate a spectral shaping multivariate LPTV filter, $\tilde{\mathbf{F}}[i, \tau]$, with period $\tilde{p}_W = 120$ (i.e., $\tilde{p} = 240$) and memory length $\tilde{m} = 4$, based on the construction of a spectral correlation profile for MIMO BB-PLC channels detailed in [20]: Let $\rho_W(\omega)$ be a 2π -periodic function representing the spectral variations in the spatial correlation. Following [20, Fig. 5], we set $\rho_W(\omega) = 0.7 - \frac{|\omega|}{2\pi}$ for $|\omega| < \pi$. Let $s[i, \omega]$ be the instantaneous PSDs, corresponding to the ‘heavily disturbed’ profile¹². Lastly, set

$$\tilde{\mathbf{F}}'[i, \omega] = \begin{bmatrix} 1 & \rho_W(\omega) \\ \rho_W(\omega) & 1 \end{bmatrix}^{1/2} \begin{bmatrix} s[i, \omega] & 0 \\ 0 & s[i, \omega] \end{bmatrix}^{1/2}.$$

The CIR of the multivariate filter $\tilde{\mathbf{F}}[i, \tau]$ is obtained via the inverse Fourier transform $\tilde{\mathbf{F}}[i, \tau] = \frac{1}{2\pi} \int_{\omega=-\pi}^{\pi} \tilde{\mathbf{F}}'[i, \omega] e^{j\omega\tau} d\omega$. Finally, the additive noise signal $\tilde{\mathbf{W}}[i] \in \mathcal{R}^2$ is obtained as the output of $\tilde{\mathbf{F}}[i, \tau]$ as in (20).

The capacity bounds for the MIMO BB-PLC channel vs. SNR, defined here as $\text{SNR} = \frac{\tilde{P}}{\frac{1}{\tilde{p}} \sum_{i=1}^{\tilde{p}} \mathbb{E}\{\|\tilde{\mathbf{W}}[i]\|^2\}}$, are depicted in Figs. 5-6 for the **MIMO GM** and for the **MIMO MCA** noise models, respectively. Similarly to the capacity of the scalar BB-PLC channel, the lower bound in (16b) is tighter than the lower bound in (16a) for almost the entire SNR range. We also note that the gap between the tighter lower bound and the upper bound in Figs. 5-6 is larger than in the scalar case in Figs. 2-4, varying from 3.05 bps/Hz at SNR of 0 dB to 0.45 bps/Hz at high SNRs for the **MIMO GM** noise model, while for the **MIMO MCA** noise model the corresponding gap varies from 4.5 bps/Hz at SNR of 0 dB to 1.1 bps/Hz at high SNRs. Comparing the capacity of MIMO BB-PLC channels in Figs. 5-6 with their scalar counterparts in Figs. 2-4, respectively, indicates that the potential rate gains of using MIMO techniques for BB-PLC can range between 40% – 90%. Recall that the optimal rate gain of a 2×2 configuration over the scalar channel for spatially independent noise is 100% [44, Ch 9]. Hence, by using two transmit ports and

¹²The instantaneous PSDs are taken from <http://www.plc.uma.es/channels.htm>, which is based on [14].

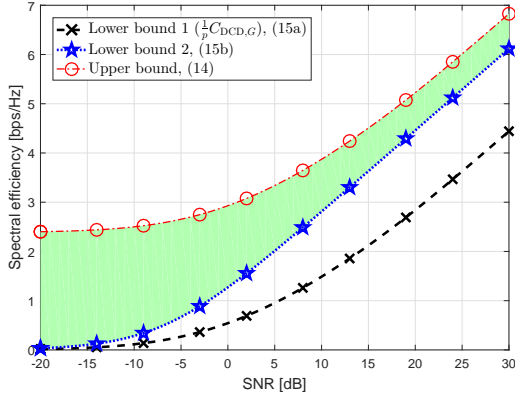


Fig. 3. Capacity bounds for the scalar BB-PLC channel, with the **GM2** noise model.

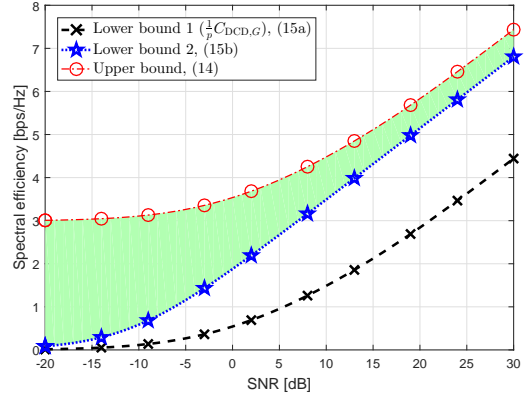


Fig. 4. Capacity bounds for the scalar BB-PLC channel, with the **MCA** noise model.

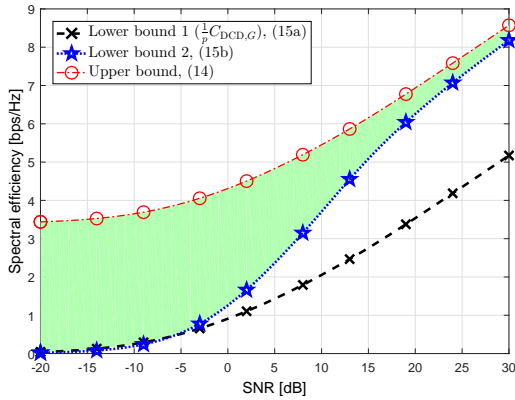


Fig. 5. Capacity bounds for the MIMO BB-PLC channel, with the **MIMO GM** noise.

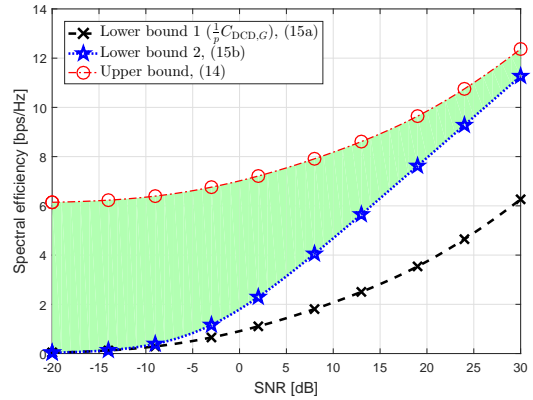


Fig. 6. Capacity bounds for the MIMO BB-PLC channel, with the **MIMO MCA** noise.

two receive ports, one can achieve gains which are close to the maximal gain. For example, at an SNR of 20 dB, we observe in Fig. 5 that the capacity of the **MIMO GM** noise channel is between 6.2 – 6.9 bps/Hz, while for the scalar case, we observe in Fig. 2 that the capacity is between 3.8 – 4 bps/Hz. Thus, the MIMO configuration can achieve a rate gain of 55% – 81% over the scalar channel. For the **MIMO MCA** noise the corresponding rate gain is 38% – 88%. This indicates that MIMO BB-PLC configurations can achieve significant rate gains over scalar BB-PLC channel at manageable computational complexity [44, Ch. 7], [39, Ch. 10]. Finally, we note that for the considered channel models, it follows from our capacity analysis that a BB-PLC system with a configuration similar to the ITU-T G.9963 standard [45], namely, a system which utilizes two transmit ports and two receive ports, over a frequency band of 100 MHz, can achieve data rates approaching and even surpassing one Gbps at high SNRs.

Our results lead to several insights on practical channel coding for BB-PLC channels: First, observe that at high SNRs for both scalar and MIMO BB-PLC channels, there is a rather

small gap between the achievable rate of cyclostationary Gaussian inputs and capacity. This indicates that at high SNR, cyclostationary Gaussian codes can closely approach the optimal performance. For lower SNR values, guidelines to a possible code construction can be obtained from the equivalence between BB-PLC channels and LNGMCs, which belong to the class of time-invariant MIMO channels, as noted in Subsection III-B. Consequently, any code for time-invariant MIMO channels, can be used in BB-PLC channels, by applying the inverse DCD to the transmitted codeword and the DCD to the channel output, achieving the same average probability of error of the code.

VI. CONCLUSIONS

In this paper we characterized upper and lower bounds on the capacity of MIMO BB-PLC channels, accounting for the unique characteristics of these channels and the non-Gaussianity of the additive noise. We derived capacity bounds which depend on the noise distribution only through its entropy rate and autocorrelation function, and obtained explicit expressions for the entropy rates of several BB-PLC noise models. Our numerical evaluations demonstrate the tightness of the proposed bounds, and illustrate the significant loss resulting from assuming that the noise is Gaussian in the computation of the capacity, which may lead to the design of inherently suboptimal schemes.

APPENDIX

A. Proof of Proposition 2

In order to prove (10), let $\mathbf{W}_G[i]$ be a zero-mean Gaussian process with an autocorrelation function $C_{\mathbf{W}}[\tau]$, defined after (8), s.t. $\mathbf{W}_G[i]$ is mutually independent of the channel input. Note that the mutual information in (6) can be written as

$$\begin{aligned} \frac{1}{n} I(\mathbf{X}^{n-1}; \mathbf{Y}^{n-1} | \mathbf{X}_{-m}^{-1} = \mathbf{0}_{n_t \cdot m}) &= \frac{1}{n} h(\mathbf{Y}^{n-1} | \mathbf{X}_{-m}^{-1} = \mathbf{0}_{n_t \cdot m}) - \frac{1}{n} h(\mathbf{W}^{n-1}) \\ &= \frac{1}{n} \left(h(\mathbf{Y}^{n-1} | \mathbf{X}_{-m}^{-1} = \mathbf{0}_{n_t \cdot m}) - h(\mathbf{W}_G^{n-1}) \right) \\ &\quad + \frac{1}{n} h(\mathbf{W}_G^{n-1}) - \frac{1}{n} h(\mathbf{W}^{n-1}). \end{aligned} \quad (\text{A.1})$$

Since, for a given correlation function, Gaussian distribution maximizes the differential entropy [27, Thm. 8.6.5], $h(\mathbf{Y}^{n-1})$ is maximized for a Gaussian distribution of \mathbf{Y}^{n-1} with the same first and second-order moments as the original vector \mathbf{Y}^{n-1} . By letting $\{\mathbf{Y}_G[i]\}_{i=0}^{n-1}$ be a Gaussian process with the same first and second-order statistical moments as $\{\mathbf{Y}[i]\}_{i=0}^{n-1}$, we have that

$$\begin{aligned}
& \lim_{n \rightarrow \infty} \frac{1}{n} \sup_{p(\mathbf{X}^{n-1}): \frac{1}{n} \sum_{i=0}^{n-1} \mathbb{E}\{\|\mathbf{X}[i]\|^2\} \leq P} h(\mathbf{Y}^{n-1} | \mathbf{X}_{-m}^{-1} = \mathbf{0}_{n_t \cdot m}) - h(\mathbf{W}_G^{n-1}) \\
& \stackrel{(a)}{\leq} \lim_{n \rightarrow \infty} \frac{1}{n} \sup_{\text{Cov}(\mathbf{X}^{n-1}): \text{Tr}(\text{Cov}(\mathbf{X}^{n-1})) \leq nP} h(\mathbf{Y}_G^{n-1} | \mathbf{X}_{-m}^{-1} = \mathbf{0}_{n_t \cdot m}) - h(\mathbf{W}_G^{n-1}) \stackrel{(b)}{=} C_G, \quad (\text{A.2})
\end{aligned}$$

where $\text{Tr}(\cdot)$ denotes the trace of a matrix, (a) follows from [27, Thm. 8.6.5], and since the differential entropy of a Gaussian random vector depends only on its covariance matrix [27, Thm. 8.4.1], hence the supremum is carried out over the covariance of the input; and (b) follows from [37, Lemma 3], noting that $h(\mathbf{Y}_G^{n-1} | \mathbf{X}_{-m}^{-1} = \mathbf{0}_{n_t \cdot m}) - h(\mathbf{W}_G^{n-1})$ denotes the mutual information between the input and the output of an LTI MIMO channel with additive Gaussian noise \mathbf{W}_G^{n-1} and Gaussian output $\mathbf{Y}_G^{n-1} = \tilde{\mathbf{G}}_n \mathbf{X}^{n-1} + \mathbf{W}^{n-1}$, as in (8). Plugging (A.1)–(A.2) into (6) yields

$$C_L < C_G + \lim_{n \rightarrow \infty} \left(\frac{1}{n} h(\mathbf{W}_G^{n-1}) - \frac{1}{n} h(\mathbf{W}^{n-1}) \right) = C_G + \bar{H}_{G, \mathbf{W}} - \bar{H}_{\mathbf{W}}, \quad (\text{A.3})$$

which proves the upper bound in (10). \square

B. Proof of Proposition 3

The bound in (11a) follows since it can be concluded from [55], [30, Thm. 7.4.3]¹³, that for a given noise covariance matrix, then Gaussian noise is the worst-case noise distribution in terms of capacity, i.e., it results in the smallest capacity. Specifically, the supremum of $I(\mathbf{X}^{n-1}; \mathbf{Y}^{n-1} | \mathbf{X}_{-m}^{-1} = \mathbf{0}_{n_t \cdot m}) = I(\mathbf{X}^{n-1}; \tilde{\mathbf{G}}_n \mathbf{X}^{n-1} + \mathbf{W}^{n-1})$ over all input distributions is lower bounded by the mutual information between the channel inputs and the channel outputs in which the additive non-Gaussian noise is replaced with an additive Gaussian noise with the same second-order moments as that of the non-Gaussian noise. Consequently, in the limit of $n \rightarrow \infty$, Eq. (11a) directly follows from (6).

Next, from (8) we note that since both \mathbf{X}^{n-1} and \mathbf{W}^{n-1} are independent of \mathbf{X}_{-m}^{-1} , then

$$h(\mathbf{Y}^{n-1} | \mathbf{X}_{-m}^{-1} = \mathbf{0}_{n_t \cdot m}) = h(\tilde{\mathbf{G}}_n \mathbf{X}^{n-1} + \mathbf{W}^{n-1}) \stackrel{(a)}{\geq} \frac{n \cdot n_r}{2} \log \left(2^{\frac{2h(\tilde{\mathbf{G}}_n \mathbf{X}^{n-1})}{n \cdot n_r}} + 2^{\frac{2h(\mathbf{W}^{n-1})}{n \cdot n_r}} \right), \quad (\text{B.1})$$

where (a) follows from the entropy power inequality [27, Thm. 17.7.3]. Thus, we have that

¹³While [30, Thm. 7.4.3] is stated for scalar channels, the same proof also applies to MIMO channels.

$$\begin{aligned}
& \sup_{p(\mathbf{X}^{n-1}): \frac{1}{n} \sum_{i=0}^{n-1} \mathbb{E}\{\|\mathbf{X}[i]\|^2\} \leq P} \frac{1}{n} I(\mathbf{X}^{n-1}; \mathbf{Y}^{n-1} | \mathbf{X}_{-m}^{-1} = \mathbf{0}_{n_t \cdot m}) \\
&= \sup_{p(\mathbf{X}^{n-1}): \frac{1}{n} \mathbb{E}\{\|\mathbf{X}^{n-1}\|^2\} \leq P} \frac{1}{n} h(\mathbf{Y}^{n-1} | \mathbf{X}_{-m}^{-1} = \mathbf{0}_{n_t \cdot m}) - \frac{1}{n} h(\mathbf{W}^{n-1}) \\
&\stackrel{(a)}{\geq} \sup_{p(\mathbf{X}^{n-1}): \frac{1}{n} \mathbb{E}\{\|\mathbf{X}^{n-1}\|^2\} \leq P} \frac{n_r}{2} \log \left(2^{\frac{2h(\tilde{\mathbf{G}}_n \mathbf{X}^{n-1})}{n \cdot n_r}} + 2^{\frac{2h(\mathbf{W}^{n-1})}{n \cdot n_r}} \right) - \frac{1}{n} h(\mathbf{W}^{n-1}), \quad (\text{B.2})
\end{aligned}$$

where (a) follows from (B.1). Note that for any positive constants a_1, a_2, a_3 and a real constant t , the function $\log(a_1 2^{a_2 t} + a_3)$ is monotonically increasing w.r.t. t , therefore

$$\begin{aligned}
& \sup_{p(\mathbf{X}^{n-1}): \frac{1}{n} \mathbb{E}\{\|\mathbf{X}^{n-1}\|^2\} \leq P} \frac{n_r}{2} \log \left(2^{\frac{2}{n \cdot n_r} h(\tilde{\mathbf{G}}_n \mathbf{X}^{n-1})} + 2^{\frac{2}{n \cdot n_r} h(\mathbf{W}^{n-1})} \right) \\
&= \frac{n_r}{2} \log \left(2^{\sup_{p(\mathbf{X}^{n-1}): \frac{1}{n} \mathbb{E}\{\|\mathbf{X}^{n-1}\|^2\} \leq P} \frac{2}{n \cdot n_r} h(\tilde{\mathbf{G}}_n \mathbf{X}^{n-1})} + 2^{\frac{2}{n \cdot n_r} h(\mathbf{W}^{n-1})} \right). \quad (\text{B.3})
\end{aligned}$$

Next, consider Eq. (B.3): Note that when $n_t = n_r$ and $\mathbf{G}[0]$ is invertible, it follows from (7) that $\tilde{\mathbf{G}}_n$ is also invertible, hence, by letting $\mathcal{M}_{n \cdot P}$ be the set of $n_t \times n_t$ positive semi-definite real symmetric matrices \mathbf{C}_X such that $\text{Tr}(\mathbf{C}_X) \leq n \cdot P$, we have that

$$\begin{aligned}
& \sup_{p(\mathbf{X}^{n-1}): \frac{1}{n} \mathbb{E}\{\|\mathbf{X}^{n-1}\|^2\} \leq P} \frac{2}{n \cdot n_r} h(\tilde{\mathbf{G}}_n \mathbf{X}^{n-1}) \stackrel{(a)}{=} \frac{2}{n \cdot n_r} \log |\tilde{\mathbf{G}}_n| + \frac{2}{n \cdot n_r} \sup_{p(\mathbf{X}^{n-1}): \frac{1}{n} \mathbb{E}\{\|\mathbf{X}^{n-1}\|^2\} \leq P} h(\mathbf{X}^{n-1}) \\
&\stackrel{(b)}{=} \frac{1}{n \cdot n_r} \log |\tilde{\mathbf{G}}_n|^2 + \frac{1}{n \cdot n_r} \sup_{\text{Cov}(\mathbf{X}^{n-1}) \in \mathcal{M}_{n \cdot P}} \log (2\pi e)^{n \cdot n_r} |\text{Cov}(\mathbf{X}^{n-1})| \\
&= \frac{1}{n \cdot n_r} \log |\tilde{\mathbf{G}}_n \tilde{\mathbf{G}}_n^T| + \log(2\pi e) + \frac{1}{n \cdot n_r} \sup_{\text{Cov}(\mathbf{X}^{n-1}) \in \mathcal{M}_{n \cdot P}} \log |\text{Cov}(\mathbf{X}^{n-1})|, \quad (\text{B.4})
\end{aligned}$$

where (a) follows from [27, Eq. (8.71)], and (b) follows from [27, Thm. 8.6.5]. Since $\text{Cov}(\mathbf{X}^{n-1})$ is positive semi-definite, it follows from the inequality of the arithmetic and geometric means [48, Pg. 326] that $|\text{Cov}(\mathbf{X}^{n-1})| \leq \left(\frac{1}{n \cdot n_t} \text{Tr}(\text{Cov}(\mathbf{X}^{n-1})) \right)^{n \cdot n_t}$, and thus $\frac{1}{n \cdot n_t} \log |\text{Cov}(\mathbf{X}^{n-1})| \leq \log \left(\frac{1}{n \cdot n_t} \text{Tr}(\text{Cov}(\mathbf{X}^{n-1})) \right)$. Consequently,

$$\begin{aligned}
\frac{1}{n \cdot n_t} \sup_{\text{Cov}(\mathbf{X}^{n-1}) \in \mathcal{M}_{n \cdot P}} \log |\text{Cov}(\mathbf{X}^{n-1})| &\leq \sup_{\text{Cov}(\mathbf{X}^{n-1}) \in \mathcal{M}_{n \cdot P}} \log \left(\frac{1}{n \cdot n_t} \text{Tr}(\text{Cov}(\mathbf{X}^{n-1})) \right) \\
&\stackrel{(a)}{\leq} \log \left(\frac{P}{n_t} \right), \quad (\text{B.5})
\end{aligned}$$

where (a) follows since $\log(\cdot)$ is monotonically increasing over \mathcal{R}^+ . Note that for $\text{Cov}(\mathbf{X}^{n-1}) = \frac{P}{n_t} \cdot \mathbf{I}_{n \cdot n_t}$ the right hand side of (B.5) is obtained with equality. Plugging this assignment into

(B.4), and recalling that $n_t = n_r$, yields

$$\begin{aligned} \sup_{p(\mathbf{X}^{n-1}): \frac{1}{n} \mathbb{E} \{ \|\mathbf{X}^{n-1}\|^2 \} \leq P} \frac{2}{n \cdot n_r} h \left(\tilde{\mathbf{G}}_n \mathbf{X}^{n-1} \right) &= \frac{1}{n \cdot n_r} \log |\tilde{\mathbf{G}}_n \tilde{\mathbf{G}}_n^T| + \log(2\pi e) + \log \left(\frac{P}{n_t} \right) \\ &= \log \left(2\pi e \frac{P}{n_t} \right) + \frac{1}{n \cdot n_r} \log |\tilde{\mathbf{G}}_n \tilde{\mathbf{G}}_n^T|. \end{aligned} \quad (\text{B.6})$$

Combining (B.6), (B.3), and (B.2) results in $\frac{1}{n} I(\mathbf{X}^{n-1}; \mathbf{Y}^{n-1} | \mathbf{X}_{-m}^{-1} = \mathbf{0}_{n_t \cdot m}) \geq \frac{n_r}{2} \log \left(\frac{2\pi e P}{n_t} \cdot 2^{\frac{1}{n \cdot n_r} \log |\tilde{\mathbf{G}}_n \tilde{\mathbf{G}}_n^T| + 2 \frac{2}{n \cdot n_r} h(\mathbf{W}^{n-1})} \right) - \frac{1}{n} h(\mathbf{W}^{n-1})$, for any input distribution satisfying $\frac{1}{n} \mathbb{E} \{ \|\mathbf{X}[i]\|^2 \} \leq P$ and for any n . Lastly, we note that in the limit as $n \rightarrow \infty$, it follows from the extension of Szego's theorem to block-Toeplitz matrices [37, Appendix A.2], [49, Thm. 5] that $\lim_{n \rightarrow \infty} \frac{1}{n} \log |\tilde{\mathbf{G}}_n \tilde{\mathbf{G}}_n^T| = \frac{1}{2\pi} \sum_{k=0}^{n_t-1} \int_{\omega=-\pi}^{\pi} \log(\alpha'_k(\omega)) d\omega$, therefore, since 2^t is continuous w.r.t. $t \in \mathcal{R}$, letting n tend to infinity in (B.2), it follows from (6) and [48, Pg. 224] that

$$\begin{aligned} C_L &\geq \lim_{n \rightarrow \infty} \frac{n_r}{2} \log \left(\frac{2\pi e P}{n_t} \cdot 2^{\frac{1}{n \cdot n_r} \log |\tilde{\mathbf{G}}_n \tilde{\mathbf{G}}_n^T| + 2 \frac{2}{n \cdot n_r} h(\mathbf{W}^{n-1})} \right) - \frac{1}{n} h(\mathbf{W}^{n-1}) \\ &= \frac{n_r}{2} \log \left(\frac{2\pi e P}{n_t} \cdot 2^{\frac{1}{2\pi \cdot n_r} \sum_{k=0}^{n_t-1} \int_{\omega=-\pi}^{\pi} \log(\alpha'_k(\omega)) d\omega + 2 \frac{2}{n_r} \bar{H}_{\mathbf{W}}} \right) - \bar{H}_{\mathbf{W}}, \end{aligned} \quad (\text{B.7})$$

which completes the proof of (11). \square

C. Proof of Theorem 1

The outline of the proof is as follows: First, in Lemma C.1 we show that the capacity of the MIMO BB-PLC channel (1), can be characterized by considering only codes whose blocklength is an integer multiple of \tilde{p} . Then, we show that the capacity of MIMO BB-PLC channels constrained to using only codes whose blocklength is an integer multiple of \tilde{p} satisfies (14).

Lemma C.1. *The capacity of the MIMO BB-PLC channel is identical to the maximum achievable rate obtained by considering only codes whose blocklength is an integer multiple of \tilde{p} .*

Proof: The proof follows by first showing that any rate achievable for the MIMO BB-PLC channel can be achieved by considering only codes whose blocklength is an integer multiple of \tilde{p} , and then showing any rate achievable for the MIMO BB-PLC channel when considering such codes, is an achievable rate for the MIMO BB-PLC channel. As these steps are essentially the same as in the proof of [56, Lemma 1], they are not repeated here. \blacksquare

Next, we note that the MIMO BB-PLC channel (1) subject to the constraint that only codes whose blocklength is an integer multiple of \tilde{p} are used, i.e., $\tilde{l} = l \cdot \tilde{p}$ where $l \in \mathcal{N}$, can be represented

as an equivalent $\tilde{p} \times \tilde{p}$ LNGMC with code blocklength l via the following assignments: Let the $\tilde{p} \cdot \tilde{n}_t \times 1$ vector $\mathbf{X}_{\text{DCD}}[i] \triangleq \tilde{\mathbf{X}}_{i \cdot \tilde{p}}^{(i+1) \cdot \tilde{p}-1}$ be the input to the transformed channel and the $\tilde{p} \cdot \tilde{n}_t \times 1$ vector $\mathbf{Y}_{\text{DCD}}[i] \triangleq \tilde{\mathbf{Y}}_{i \cdot \tilde{p}}^{(i+1) \cdot \tilde{p}-1}$ be the output of the channel. The transformation is clearly bijective as for the BB-PLC channel we consider only codes whose blocklength is an integer multiple of \tilde{p} . For each blocklength l , the input to the equivalent LNGMC satisfies

$$\frac{1}{l} \sum_{i=0}^{l-1} \mathbb{E} \left\{ \|\mathbf{X}_{\text{DCD}}[i]\|^2 \right\} = \frac{1}{l} \sum_{i=0}^{l-1} \sum_{k=0}^{\tilde{p}-1} \mathbb{E} \left\{ \left\| \tilde{\mathbf{X}}[i \cdot \tilde{p} + k] \right\|^2 \right\} = \frac{\tilde{p}}{l} \sum_{\tilde{i}=0}^{\tilde{l}-1} \mathbb{E} \left\{ \left\| \tilde{\mathbf{X}}[\tilde{i}] \right\|^2 \right\} \stackrel{(a)}{\leq} \tilde{p} \cdot \tilde{P},$$

where (a) follows from (2). Consequently, the equivalent LNGMC input is subject to a maximal power constraint $P_{\text{DCD}} = \tilde{p} \cdot \tilde{P}$. Next, we note that the input-output relationship of the BB-PLC channel (1) implies that the input-output relationship of the transformed channel is given by (12), and that the equivalent LNGMC noise $\mathbf{W}_{\text{DCD}}[i]$ appearing in (12), is a zero-mean strict-sense stationary process. Moreover, as $\tilde{p} > \tilde{m}$, it follows that the temporal dependence of $\mathbf{W}_{\text{DCD}}[i]$ spans an interval of length $m=1$. Recall that C_{DCD} denotes the capacity of the channel (12)–(13).

As each channel use in the equivalent LNGMC (12)–(13) corresponds to \tilde{p} channel uses in the BB-PLC channel (1)–(2), it follows that the maximal achievable rate of the BB-PLC channel, measured in bits per channel use, subject to the restriction that only codes whose blocklength is an integer multiple of \tilde{p} are allowed, can be obtained from the maximal achievable rate of the equivalent LNGMC as $C_{\text{PLC}} = \frac{1}{\tilde{p}} C_{\text{DCD}}$. Finally, from Lemma C.1, we conclude that C_{PLC} is the maximum achievable rate for the BB-PLC channel, thus proving the theorem. \square

D. Proof of Proposition 4

In order to derive the differential entropy of complex Nakagami- m RVs, we use the following lemma, which states the PDF of a family of complex RVs:

Lemma D.1. *Let W be a complex RV given by $W = X e^{j\Theta}$, where X is a non-negative real RV, and Θ is an RV uniformly distributed over $[0, 2\pi]$, mutually independent of X , then, the PDF of W is given by $f_W(w) = \frac{f_X(|w|)}{2\pi|w|}$, and its differential entropy is given by*

$$h(W) = \log(2\pi) + \mathbb{E} \left\{ \log(X) \right\} + h(X). \quad (\text{D.1})$$

Proof: Let $W_{\text{R}}, W_{\text{I}}$ be the real and imaginary parts of W , respectively, and recall that the PDF of a complex RV $W = W_{\text{R}} + jW_{\text{I}}$ is given by $f_W(w = w_{\text{R}} + jw_{\text{I}}) = f_{W_{\text{R}}, W_{\text{I}}}(w_{\text{R}}, w_{\text{I}})$ [52, Pg. 188]. Consequently, letting $\arg(z)$ denote the phase of a complex number z , the PDF $f_{W_{\text{R}}, W_{\text{I}}}(w_{\text{R}}, w_{\text{I}})$ is obtained using the transformation of RVs theorem as in [52, Pg. 146]:

$$f_{W_R, W_I}(w_R, w_I) = \frac{f_{X, \Theta}\left(\sqrt{w_R^2 + w_I^2}, \arg\left(\frac{w_I}{w_R}\right)\right)}{\sqrt{w_R^2 + w_I^2}} \stackrel{(a)}{=} \frac{f_X\left(\sqrt{w_R^2 + w_I^2}\right)}{2\pi\sqrt{w_R^2 + w_I^2}} = \frac{f_X(|w|)}{2\pi|w|}, \quad (\text{D.2})$$

where (a) follows since X and Θ are mutually independent, thus $f_{X, \Theta}(x, \theta) = f_X(x) f_\Theta(\theta)$, and from the uniform distribution of Θ . It thus follows that $f_W(w) = \frac{f_X(|w|)}{2\pi|w|}$.

Using (D.2), we next derive the differential entropy of W as:

$$\begin{aligned} h(W) &= - \int_{\mathcal{R}^2} \frac{f_X\left(\sqrt{w_R^2 + w_I^2}\right)}{2\pi\sqrt{w_R^2 + w_I^2}} \log\left(\frac{f_X\left(\sqrt{w_R^2 + w_I^2}\right)}{2\pi\sqrt{w_R^2 + w_I^2}}\right) dw_R dw_I \\ &\stackrel{(a)}{=} - \int_{\theta=0}^{2\pi} \int_{x=0}^{\infty} x \frac{f_X(x)}{2\pi x} \log\left(\frac{f_X(x)}{2\pi x}\right) dx d\theta = - \int_{x=0}^{\infty} f_X(x) \log\left(\frac{f_X(x)}{2\pi x}\right) dx, \end{aligned} \quad (\text{D.3})$$

where (a) is obtained by switching the integration variables from (w_R, w_I) to (x, θ) , given by $x = \sqrt{w_R^2 + w_I^2}$ and $\theta = \tan^{-1}\left(\frac{w_I}{w_R}\right)$. Note that (D.3) can be written as

$$\begin{aligned} - \int_{x=0}^{\infty} f_X(x) \log\left(\frac{f_X(x)}{2\pi x}\right) dx &= \int_{x=0}^{\infty} f_X(x) \log(2\pi) dx + \int_{x=0}^{\infty} f_X(x) \log(x) dx - \int_{x=0}^{\infty} f_X(x) \log(f_X(x)) dx \\ &= \log(2\pi) + \mathbb{E}\{\log(X)\} + h(X). \end{aligned} \quad (\text{D.4})$$

Plugging (D.4) into (D.3) we obtain (D.1). ■

For a complex Nakagami- m RV W , we have that the PDF of X is given by (17). Plugging the PDF (17) into (D.2) we obtain the PDF of W as: $f_W(w) = \frac{2}{2\pi\Gamma(m)} \left(\frac{m}{\Omega}\right)^m |w|^{2m-2} e^{-\frac{m|w|^2}{\Omega}}$. To obtain the differential entropy of the complex Nakagami- m RV $W = X e^{j\Theta}$, we note that for $X \sim \mathcal{KG}(m, \Omega)$, $\mathbb{E}\{\log(X)\} = \int_{x=0}^{\infty} \frac{2}{\Gamma(m)} \left(\frac{m}{\Omega}\right)^m x^{2m-1} e^{-\frac{mx^2}{\Omega}} \log(x) dx$. Setting $t \triangleq \frac{mx^2}{\Omega}$ as the integration variable, we have $dt = 2\frac{mx}{\Omega} dx$, $\log(t) = \log\left(\frac{m}{\Omega}\right) + 2\log(x)$, and $x^2 = \frac{\Omega}{m}t$, resulting in:

$$\begin{aligned} \mathbb{E}\{\log(X)\} &= \int_{t=0}^{\infty} \frac{1}{2\Gamma(m)} t^{m-1} e^{-t} \left(\log(t) - \log\left(\frac{m}{\Omega}\right) \right) dt \\ &= \frac{1}{2\ln(2)} \int_{t=0}^{\infty} \frac{1}{\Gamma(m)} t^{m-1} e^{-t} \ln(t) dt - \frac{1}{2\Gamma(m)} \log\left(\frac{m}{\Omega}\right) \int_{t=0}^{\infty} t^{m-1} e^{-t} dt \\ &\stackrel{(a)}{=} \frac{1}{2\ln(2)} \Psi(m) - \frac{1}{2} \log\left(\frac{m}{\Omega}\right), \end{aligned} \quad (\text{D.5})$$

where (a) follows since $\Psi(x) = \frac{d}{dx}\left(\ln(\Gamma(x))\right) = \frac{1}{\Gamma(x)} \int_{t=0}^{\infty} t^{x-1} e^{-t} \ln(t) dt$ [53, Tbl. 0.1]. Next, recall that the differential entropy of a real-valued Nakagami- m RV is given by [53, Ch. 4.18]:

$h(X) = \log\left(\frac{\Gamma(m)}{2} \sqrt{\frac{\Omega}{m}} e^{\frac{2m-(2m-1)\Psi(m)}{2}}\right)$. Plugging this and (D.5) into (D.1), we have that

$$\begin{aligned} h(W) = h(W_R, W_I) &= \log(2\pi) + \frac{1}{2\ln(2)}\Psi(m) - \frac{1}{2}\log\left(\frac{m}{\Omega}\right) + \log\left(\frac{\Gamma(m)}{2} \sqrt{\frac{\Omega}{m}} e^{\frac{2m-(2m-1)\Psi(m)}{2}}\right) \\ &= \frac{1}{2\ln(2)}\Psi(m) + \log\left(\frac{\pi\Omega}{m}\Gamma(m)e^{\frac{2m-(2m-1)\Psi(m)}{2}}\right), \end{aligned} \quad (\text{D.6})$$

proving the proposition. \square

E. Proof of Lemma 1

To prove Lemma 1, we first state Lemma E.1, which characterizes a relationship between the entropy rate of an i.i.d. process $\mathbf{U}[i]$, $\bar{H}_{\mathbf{U}} = h(\mathbf{U})$, and the entropy rate of $\mathbf{W}[i]$, $\bar{H}_{\mathbf{W}}$, obtained by LTI filtering of $\mathbf{U}[i]$:

Lemma E.1. *Let $\mathbf{U}[i] \in \mathcal{R}^{n_r}$ be an i.i.d. multivariate process, $\{\mathbf{F}[\tau]\}_{\tau=0}^m$ be a set of $n_r \times n_r$ matrices s.t. $\mathbf{F}[0]$ is non-singular. Define $\mathbf{W}[i] = \sum_{\tau=0}^m \mathbf{F}[\tau]\mathbf{U}[i-\tau]$, and $\mathbf{F}'(\omega) \triangleq \sum_{\tau=0}^m \mathbf{F}[\tau]e^{-j\omega\tau}$, and let $\bar{H}_{\mathbf{W}}$ and $\bar{H}_{\mathbf{U}}$ denote the entropy rates of $\mathbf{W}[i]$ and $\mathbf{U}[i]$, respectively. Then, we have*

$$\bar{H}_{\mathbf{W}} = \frac{1}{2\pi} \int_{\omega=0}^{2\pi} \log |\mathbf{F}'(\omega)| d\omega + \bar{H}_{\mathbf{U}}. \quad (\text{E.1})$$

Comment E.1. For $n_r = 1$, (E.1) specializes the entropy gain of scalar filters in [54, Thm. 14].

Proof: Since we are interested in the entropy rate we may assume that the blocklengths are sufficiently large and consider $n > 2m$. Define the $n \cdot n_r \times n \cdot n_r$ matrix $\tilde{\mathbf{F}}_n^a$, the $m \cdot n_r \times m \cdot n_r$ matrix $\tilde{\mathbf{F}}_m^b$, and the $n \cdot n_r \times m \cdot n_r$ matrix $\tilde{\mathbf{F}}_n^c$, via

$$\tilde{\mathbf{F}}_n^a \triangleq \begin{bmatrix} \mathbf{F}[0] & \cdots & 0 & \cdots & 0 \\ \vdots & \ddots & & \ddots & \vdots \\ \mathbf{F}[m] & \cdots & \mathbf{F}[0] & \cdots & 0 \\ \vdots & \ddots & & \ddots & \vdots \\ 0 & \cdots & \mathbf{F}[m] & \cdots & \mathbf{F}[0] \end{bmatrix}, \quad \tilde{\mathbf{F}}_m^b \triangleq \begin{bmatrix} \mathbf{F}[m] & \cdots & \mathbf{F}[1] \\ \vdots & \ddots & \vdots \\ 0 & \cdots & \mathbf{F}[m] \end{bmatrix}, \quad \tilde{\mathbf{F}}_n^c \triangleq \begin{bmatrix} & \tilde{\mathbf{F}}_m^b & \\ \mathbf{0}_{(n-m) \cdot n_r \times m \cdot n_r} & & \end{bmatrix}. \quad (\text{E.2})$$

Note that $\tilde{\mathbf{F}}_n^a$ is block-Toeplitz and non-singular (hence, invertible), as $\mathbf{F}[0]$ is non-singular. Using (E.2), we can write $\mathbf{W}^{n-1} = \tilde{\mathbf{F}}_n^a \mathbf{U}^{n-1} + \tilde{\mathbf{F}}_n^c \mathbf{U}_{-m}^{-1} = \tilde{\mathbf{F}}_n^e \mathbf{U}^{n-1}$. As $\mathbf{U}[i]$ is i.i.d., then $\tilde{\mathbf{F}}_n^a \mathbf{U}^{n-1}$ and $\tilde{\mathbf{F}}_n^c \mathbf{U}_{-m}^{-1}$ are mutually independent. Hence, $h\left(\mathbf{W}^{n-1} | \tilde{\mathbf{F}}_n^c \mathbf{U}_{-m}^{-1}\right) = h\left(\tilde{\mathbf{F}}_n^a \mathbf{U}^{n-1}\right)$, and we can write

$$\begin{aligned}
h(\mathbf{W}^{n-1}) - h(\tilde{\mathbf{F}}_n^a \mathbf{U}^{n-1}) &= I(\tilde{\mathbf{F}}_n^c \mathbf{U}_{-m}^{-1}; \mathbf{W}^{n-1}) \stackrel{(a)}{=} I(\tilde{\mathbf{F}}_m^b \mathbf{U}_{-m}^{-1}; \mathbf{W}^{n-1}) \quad (\text{E.3}) \\
&= I(\tilde{\mathbf{F}}_m^b \mathbf{U}_{-m}^{-1}; \tilde{\mathbf{F}}_n^a \mathbf{U}^{n-1} + \tilde{\mathbf{F}}_n^c \mathbf{U}_{-m}^{-1}) = h(\tilde{\mathbf{F}}_m^b \mathbf{U}_{-m}^{-1}) - h(\tilde{\mathbf{F}}_m^b \mathbf{U}_{-m}^{-1} | \tilde{\mathbf{F}}_n^a \mathbf{U}^{n-1} + \tilde{\mathbf{F}}_n^c \mathbf{U}_{-m}^{-1}) \\
&\stackrel{(b)}{\leq} h(\tilde{\mathbf{F}}_m^b \mathbf{U}_{-m}^{-1}) - h(\tilde{\mathbf{F}}_m^b \mathbf{U}_{-m}^{-1} | \tilde{\mathbf{F}}_n^a \mathbf{U}^{n-1} + \tilde{\mathbf{F}}_n^c \mathbf{U}_{-m}^{-1}, \mathbf{U}_m^{n-1}) \\
&\stackrel{(c)}{=} h(\tilde{\mathbf{F}}_m^b \mathbf{U}_{-m}^{-1}) - h(\tilde{\mathbf{F}}_m^b \mathbf{U}_{-m}^{-1} | \tilde{\mathbf{F}}_{2m}^a \mathbf{U}^{2m-1} + \tilde{\mathbf{F}}_{2m}^c \mathbf{U}_{-m}^{-1}, \mathbf{U}_m^{n-1}) \\
&\stackrel{(d)}{=} h(\tilde{\mathbf{F}}_m^b \mathbf{U}_{-m}^{-1}) - h(\tilde{\mathbf{F}}_m^b \mathbf{U}_{-m}^{-1} | \tilde{\mathbf{F}}_{2m}^a \mathbf{U}^{2m-1} + \tilde{\mathbf{F}}_{2m}^c \mathbf{U}_{-m}^{-1}, \mathbf{U}_m^{2m-1}) \\
&= I(\tilde{\mathbf{F}}_m^b \mathbf{U}_{-m}^{-1}; \tilde{\mathbf{F}}_{2m}^a \mathbf{U}^{2m-1} + \tilde{\mathbf{F}}_{2m}^c \mathbf{U}_{-m}^{-1}, \mathbf{U}_m^{2m-1}) = I(\tilde{\mathbf{F}}_m^b \mathbf{U}_{-m}^{-1}; \mathbf{W}^{2m-1}, \mathbf{U}_m^{2m-1}), \quad (\text{E.4})
\end{aligned}$$

where (a) follows from the definition of $\tilde{\mathbf{F}}_n^c$ in (E.2); and (b) follows as conditioning decreases the entropy; in (c) the matrix $\tilde{\mathbf{F}}_{2m}^a$ is an $2m \cdot n_r \times 2m \cdot n_r$ matrix in which each row consists of the first $2m$ elements of the corresponding row of $\tilde{\mathbf{F}}_n^a$, and $\tilde{\mathbf{F}}_{2m}^c$ is a matrix which consists of the first $2m$ rows of $\tilde{\mathbf{F}}_n^c$. Lastly, (d) follows as $\mathbf{U}[\tilde{i}]$ is an i.i.d. sequence. Noting that Eq. (E.3) implies that $h(\mathbf{W}^{n-1}) \geq h(\tilde{\mathbf{F}}_n^a \mathbf{U}^{n-1})$, we have that

$$0 \leq h(\mathbf{W}^{n-1}) - h(\tilde{\mathbf{F}}_n^a \mathbf{U}^{n-1}) \stackrel{(a)}{\leq} I(\tilde{\mathbf{F}}_m^b \mathbf{U}_{-m}^{-1}; \mathbf{W}^{2m-1}, \mathbf{U}_m^{2m-1}), \quad (\text{E.5})$$

where (a) follows from (E.4). Observing that the right hand side of (E.5) is a finite value which does not depend on n , then, dividing both sides of (E.3) by n and letting n tend to infinity yields $\lim_{n \rightarrow \infty} \frac{1}{n} h(\mathbf{W}^{n-1}) - \lim_{n \rightarrow \infty} \frac{1}{n} h(\tilde{\mathbf{F}}_n^a \mathbf{U}^{n-1}) = 0$. Therefore,

$$\bar{H}_{\mathbf{W}} = \lim_{n \rightarrow \infty} \frac{1}{n} h(\tilde{\mathbf{F}}_n^a \mathbf{U}^{n-1}) \stackrel{(a)}{=} \lim_{n \rightarrow \infty} \left(\frac{1}{n} \log |\tilde{\mathbf{F}}_n^a| + \frac{1}{n} h(\mathbf{U}^{n-1}) \right) \stackrel{(b)}{=} \frac{1}{2\pi} \int_{\theta=0}^{2\pi} \log |F'(\theta)| d\theta + \bar{H}_{\mathbf{U}},$$

where (a) follows from [27, Eq. (8.71)] as $\tilde{\mathbf{F}}_n^a$ is invertible, and (b) follows from the extension of Szegő's theorem to block-Toeplitz matrices [49, Thm. 5]. ■

Since by (21), $\mathbf{W}_{\text{DCD}}[\tilde{i}]$ is the output of an LTI filter with i.i.d. input $\mathbf{U}[\tilde{i}]$, and as that the entropy rate of $\mathbf{U}[\tilde{i}]$ is given by $\tilde{p} \cdot h(\tilde{\mathbf{U}})$, it follows from Lemma E.1 that $\bar{H}_{\mathbf{W}_{\text{DCD}}} = \frac{1}{2\pi} \int_{\omega=0}^{2\pi} \log |F'(\omega)| d\omega + \tilde{p} \cdot h(\tilde{\mathbf{U}})$, proving the lemma. □

REFERENCES

- [1] H. C. Ferreira, L. Lampe, J. Newbury, and T. G. Swart. *Power Line Communications - Theory and Applications for Narrowband and Broadband Communications over Power Lines*. Wiley and Sons, Ltd., 2010.
- [2] C. Cano, A. Pittolo, D. Malone, L. Lampe, A. M. Tonello, and A. G. Dabak. "State of the art in power line communications: From the applications to the medium," *IEEE J. Sel. A. Commun.*, vol. 34, no. 7, Jul. 2016, pp. 1935–1952.
- [3] L. T. Berger, A. Schwager, P. Pagani, and D. M. Schneider. "MIMO power line communications," *IEEE Commun. Surveys & Tutorials*, vol. 17, no. 1, Q1 2015, pp. 106–124.

- [4] H. Meng, Y. L. Guan, and S. Chen. "Modeling and analysis of noise effects on broadband power-line communications," *IEEE Trans. Power Del.*, vol. 20, no. 2, Apr. 2005, pp. 630 – 637.
- [5] A. Mathur and M. R. Bhatnagar. "PLC performance analysis assuming BPSK modulation over Nakagami-m additive noise," *IEEE Commun. Lett.*, vol. 18, no. 6, Jun. 2014, pp. 909 – 912.
- [6] A. Mathur, M. R. Bhatnagar, and B. K. Panigrahi. "Performance evaluation of PLC Under the combined effect of background and impulsive noises," *IEEE Commun. Lett.*, vol. 19, no. 7, Jul. 2015, pp. 1117 – 1120.
- [7] W. Bo, Q. Yinghao, H. Peiwei, and C. Wenhao. "Indoor powerline channel simulation and capacity analysis," *IET Conference on Wireless, Mobile Sensor Networks*, Shanghai, China, Dec. 2007, pp. 154-156.
- [8] F. Gianaroli, F. Pancaldi, and G. M. Vitetta. "The impact of statistical noise modeling on the error-rate performance of OFDM power-line communications," *IEEE Trans. Power Del.*, vol. 29, no. 6, Apr. 2014, pp. 2622 – 2630.
- [9] M. Gotz, M. Rapp, and K. Dostert. "Power line channel characteristics and their effect on communication system design," *IEEE Commun. Mag.*, vol. 42, no. 4, Apr. 2004, pp. 78 – 86.
- [10] A. M. Tonello, F. Versolatto, and A. Pittolo. "In-home power line communication channel: Statistical characterization," *IEEE Trans. Commun.*, vol. 62, no. 6, Jun. 2014, pp. 2096 – 2106.
- [11] T. Esmailian, F. R. Kschischang, and P. Glenn Gulak. "In-building power lines as high-speed communication channels: channel characterization and a test channel ensemble," *Int. J. Commun. Sys.*, vol. 16, no. 5, May 2003, pp. 381-400.
- [12] S. Galli. "A novel approach to the statistical modeling of wireline channels," *IEEE Trans. Commun.*, vol. 59, no. 5, May 2011, pp. 1332-1345.
- [13] F. J. Cañete, J. A. Cortés, L. Díez, and J. T. Entrambasaguas. "Analysis of the cyclic short-term variation of indoor power line channels," *IEEE J. Sel. A. Commun.*, vol. 24, no. 7, Jul. 2006, pp. 1327–1338.
- [14] J. A. Cortés, L. Díez, F. J. Cañete, and J. J. Sánchez-Martínez. "Analysis of the indoor broadband power-line noise scenario," *IEEE Trans. Electromagn. Compat.*, vol. 52, no. 4, Nov. 2010, pp. 849–858.
- [15] M. Zimmermann and K. Dostert. "Analysis and modeling of impulsive noise in broad-band powerline communications," *IEEE Trans. Electromagn. Compat.*, vol. 44, no. 1, Feb. 2002, pp. 249–258.
- [16] Y. H. Ma, P. L. So, and E. Gunawan. "Performance analysis of OFDM systems for broadband power line communications under impulsive noise and multipath effects," *IEEE Trans. Power Del.*, vol. 20, no. 2, Apr. 2005, pp. 674–681.
- [17] M. Zimmermann and K. Dostert. "A multipath model for the powerline channel," *IEEE Trans. Commun.*, vol. 50, no. 4, Apr. 2002, pp. 553–559.
- [18] F. Gianaroli, F. Pancaldi, and G. M. Vitetta. "On the use of Zadeh's series expansion for modeling and estimation of indoor powerline channels," *IEEE Trans. Commun.*, vol. 62, no. 7, Jul. 2014, pp. 2558–2568.
- [19] F. J. Cañete, J. A. Cortés, L. Díez, and J. T. Entrambasaguas. "A channel model proposal for indoor power line communications," *IEEE Commun. Mag.*, vol. 49, no. 12, Dec. 2011, pp. 166–174.
- [20] D. Rende, A. Nayagam, K. Afkhamie, L. Yonge, R. Riva, D. Veronesi, F. Osnato, and P. Bisaglia. "Noise correlation and its effect on capacity of inhome MIMO power line channels," *IEEE International Symposium on Power-Line Communications and its Applications (ISPLC)*, Udine, Italy, Apr. 2011, pp. 60–65.
- [21] P. Pagani and A. Schwager. "A statistical model of the in-home MIMO PLC channel based on European field measurements," *IEEE J. Sel. A. Commun.*, vol. 34, no. 7, Jul. 2016, pp. 2033–2044.
- [22] D. Veronesi, R. Riva, P. Bisaglia, F. Osnato, K. Afkhamie, A. Nayagam, D. Rende, and L. Yonge. "Characterization of in-home MIMO power line channels," *IEEE International Symposium on Power-Line Communications and its Applications (ISPLC)*, Udine, Italy, Apr. 2011, pp. 42–47.
- [23] J. A. Corchado, J. A. Cortés, F. J. Cañete, A. Arregui, and L. Díez. "Analysis of the spatial correlation of indoor MIMO PLC channels," *IEEE Commun. Letters*, vol. 21, no. 1, Jan. 2017, pp. 40–43.
- [24] D. Middleton. "Statistical-physical models of electromagnetic interference," *IEEE Trans. Electromagn. Compat.*, vol. 19, no. 3, Aug. 1977, pp. 106 – 127.
- [25] M. Nassar, K. Gulati, Y. Mortazavi, and B. L. Evans. "Statistical modeling of asynchronous impulsive noise in powerline communication networks," *IEEE Global Communications Conference (GLOBECOM)*, Houston, TX, Dec. 2011.
- [26] M. A. Tunc, E. Perrins, and L. Lampe. "Optimal LPTV-aware bit loading in broadband PLC," *IEEE Trans. Commun.*, vol. 61, no. 12, Dec. 2013, pp. 5152–5162.
- [27] T. M. Cover and J. A. Thomas. *Elements of Information Theory*. Wiley Press, 2006.
- [28] D. A. Le, H. V. Vu, N. H. Tran, M. C. Gursoy, T. Le-Ngoc. "Approximation of achievable rates in additive Gaussian mixture noise channels," *IEEE Trans. Commun.*, vol. 64, no. 23, Dec. 2016, pp. 5011 - 5024.
- [29] N. Shlezinger and R. Dabora. "On the capacity of narrowband PLC channels," *IEEE Trans. Commun.*, vol. 63, no. 4, Apr. 2015, pp. 1191 - 1201.
- [30] R. G. Gallager. *Information Theory and Reliable Communication*. Wiley and Sons, Ltd., 1968.

- [31] A. Goldsmith and M. Effros. “The capacity region of broadcast channels with intersymbol interference and colored Gaussian noise,” *IEEE Trans. Inform. Theory*, vol. 47, no. 1, Jan. 2001, pp. 219–240.
- [32] H. Weingarten, Y. Steinberg, and S. Shamai, “The capacity region of the Gaussian multiple-input multiple-output broadcast channel,” *IEEE Trans. Inform. Theory*, vol. 52, no. 9, Sep. 2006, pp. 3936–3964.
- [33] R. L. Dobrushin. “General formulation of Shannons main theorem in information theory,” *Amer. Math. Soc. Translations: Series 2*, vol. 33, 1963, pp. 323–438.
- [34] I. P. Tsaregradskii. “A note on the capacity of a stationary channel with finite memory,” *Theory of Probability and its Applications*, vol. 3, no. 1, 1958, pp. 79–91.
- [35] T. S. Han. *Information-Spectrum Methods in Information Theory*. Springer, 2003.
- [36] W. Hirt and J. L. Massey. “Capacity of discrete-time Gaussian channel with intersymbol interference,” *IEEE Trans. Inform. Theory*, vol. 34, no. 3, May 1988, pp. 380–388.
- [37] L. H. Brandenburg and A. D. Wyner. “Capacity of the Gaussian channel with memory: The multivariate case,” *Bell System Technical Journal*, vol. 53, no. 5, May. 1974, pp. 745-778.
- [38] S. Verdú. “The capacity region of the symbol-asynchronous Gaussian multiple-access channel,” *IEEE Trans. Inform. Theory*, vol. 35, no. 4, Aug. 1989, pp. 733–751.
- [39] A. Goldsmith. *Wireless Communications*. Cambridge, 2005.
- [40] J. Lin, M. Nassar, and B. L. Evans. “Impulsive noise mitigation in powerline communications using sparse Bayesian learning,” *IEEE J. Sel. A. Commun.*, vol. 31, no. 7, Jul. 2013, pp. 1172–1183.
- [41] L. Lampe, A. M. Tonello, and T. G. Swart. *Power line communications: Principles, standards and applications from multimedia to smart grid*. Wiley press, 2016.
- [42] G. B. Giannakis. “Cyclostationary signal analysis,” *Digital Signal Processing Handbook*, CRC Press, 1998, pp. 17.1–17.31.
- [43] O. C. Schrempf, O. Feiermann, and U.D. Hanebeck. “Optimal mixture approximation of the product of mixtures,” *IEEE International Conference on Information Fusion*, Philadelphia, PA, Jul. 2005.
- [44] D. Tse and P. Viswanath. *Fundamentals of Wireless Communication*. Cambridge, 2005.
- [45] International Telecommunications Union (ITU). “ITU-T Recommendation G.9963, Unified high-speed wire-line based home networking transceivers Multiple Input/Multiple Output (MIMO),” Sep. 2011.
- [46] M. Nassar, J. Lin, Y. Mortazavi, A. Dabak, I. H. Kim, and B. L. Evans. “Local utility power line communications in the 3–500 kHz band: Channel impairments, noise, and standards,” *IEEE Signal Processing Magazine*, vol. 29, no. 5, Aug. 2012, pp. 116-127.
- [47] *Appendix for Noise Channel Modeling for IEEE P1901.2*, IEEE Standard P1901.2, Jun. 2011.
- [48] H. Amann and J. Escher. *Analysis I*. Birkhauser Verlag, Basel, 2005.
- [49] J. Gutiérrez-Gutiérrez and P. M. Crespo. “Asymptotically equivalent sequences of matrices and hermitian block toeplitz matrices with continuous symbols: Applications to MIMO systems,” *IEEE Trans. Inform. Theory*, vol. 54, no. 12, Dec. 2008, pp. 5671–5680.
- [50] M. F. Huber, T. Bailey, H. Durrant-Whyte, and U. D. Hanebeck. “On entropy approximation for Gaussian mixture random vectors,” *IEEE International Conference on Multisensor Fusion and Integration for Intelligent Systems (MFI)*, Seoul, South Korea, Aug. 2008, pp. 181-188.
- [51] C. D. Meyer. *Matrix Analysis and Applied Linear Algebra*. Society for Industrial and Applied Mathematics, 2000.
- [52] A. Papoulis. *Probability, Random Variables, and Stochastic Processes*. McGraw-Hill, 1991.
- [53] J. V. Michalowicz and J. M. Nichols. *Handbook of differential entropy*. CRC press, 2013.
- [54] C. E. Shannon. “A mathematical theory of communication,” *Bell System Technical Journal*, vol. 27, no. 3-4, Jul./Oct. 1948, pp. 379-423, 623-656.
- [55] S. N. Diggavi and T. M. Cover. “The worst additive noise under a covariance constraint,” *IEEE Trans. Inform. Theory*, vol. 47, no. 7, Dec. 2001, pp. 3072–3081.
- [56] N. Shlezinger and R. Dabora. “The capacity of discrete-time Gaussian MIMO channels with periodic characteristics,” *IEEE International Symposium on Information Theory (ISIT)*, Barcelona, Spain, Jun. 2016.
- [57] *IEEE Standard for Broadband over Power Line Networks: Medium Access Control and Physical Layer Specifications*, IEEE Standard P1901-2010, Dec. 2010.